SN Computer Science (2024) 5:166
https://doi.org/10.1007/s42979-023-02472-y

ORIGINAL RESEARCH

Disturbance Rejection in the Cerebellum

Mireille Broucke[1]

Received: 9 February 2022 / Accepted: 3 November 2023

Abstract
This paper further explores the hypothesis, put forward in our earlier work, that the cerebellum performs disturbance rejection to meet the requirements of the internal model principle of control theory. We review some of the relevant experimental results that suggest such an interpretation is possible. We also discuss in an informal non-mathematical way how a model of the cerebellum for disturbance rejection may be formulated using ideas from control theory. Based on our study of the slow eye movement systems as well as visuomotor adaptation, several themes emerge, including a possible structural model of the cerebellum, and insights on how the cerebellum may enable and disable internal models. Implications for robotics are discussed at the end of the paper.

Keywords Cerebellum · Disturbance rejection · Internal model principle · Motor control

Introduction

This paper explores the hypothesis that the primary function of the cerebellum is *disturbance rejection* of exogenous reference and disturbance signals. This interpretation of cerebellar function places the *internal model principle* of control theory at front and center; that is, *any good controller must contain an internal model of its environment* [1]. The reader may notice a stylistic shift from many writings in neuroscience that treat internal models as a theoretical possibility. If the measurement structure of the brain imposes that mathematically the internal model principle must hold, then we regard this fact as inviolable, like a law of physics. The mathematical certainty of the internal model principle can be a guide in making deductions that we find are not always available if one adopts a purely empirical stance.

The idea to interpret the cerebellum in terms of disturbance rejection is, in some sense, not new. The first proposal by Stephen Lisberger on the role of internal models in the cerebellum in his survey paper [2] is consistent with a role of disturbance rejection. Lisberger describes internal models as providing "a model of the inertia of real-world objects in motion"; see also [3, 4]. Reference signals such as target motion impinge on sensory error signals in a mathematically indistinguishable way from disturbance signals. Lisberger's description of the role of internal models can be interpreted as the removal of a disturbance (the motion of a visual target) from an error signal recorded in the brain, the displacement from the fovea to the target on the retina. Motivated by findings primarily regarding the oculomotor system and by our interpretation of cerebellar function in terms of disturbance rejection, we have applied *regulator theory* [5] to form mathematical models of motor systems under regulation by the cerebellum [6–10].

The paper is informal. We suppress mathematical details as much as we can. We draw connections between different scientific subjects that are perhaps not often compared side by side: regulator designs for disturbance rejection compared with a systems-level structural model of the cerebellum; specific models of motor systems compared with each other; and comparisons between continuous-time and discrete-time processes both associated with the cerebellum. In making this survey, several themes or takeaways emerge, that we summarize here for the reader who is interested in the main points (meanings of specific terms are found in the main text below):

This article is part of the topical collection "Informatics in Control, Automation and Robotics" guest edited by Kurosh Madani, Oleg Gusikhin and Henk Nijmeijer.

✉ Mireille Broucke
broucke@control.utoronto.ca

[1] Electrical and Computer Engineering, University of Toronto, 10 King's College Rd., Toronto, ON M5S 3G4, Canada

Published online: 08 January 2024

- The structural architecture of the cerebellum resembles that of an *adaptive observer* [11, 12] or an *adaptive filter* [13–15].
- The *nucleo-cortical pathway* [16, 17] is in direct correspondence with the internal model principle in the sense that without this pathway, the internal model principle would not be satisfied by the mathematical model.
- The theory suggests that the *granular layer* filters of the cerebellum must synchronize on the same time constants for filtering *mossy fiber* (MF) inputs to the same cerebellar modules.
- Mathematically speaking, there is considerable flexibility in terms of how MF inputs to the cerebellum may be combined or "pre-bundled".
- The mathematical models suggest that some MF inputs may have the role to ensure that they are not cancelled out by the cerebellum. This seemingly contradictory role could potentially lead to misinterpretations of the function of certain cerebellar modules. On the other hand, the collaborative role between the cerebellum and feedforward signals is well known [18].
- The cerebellum may well be the unique brain structure that is wired to handle the dangerous operation of shutting on and off internal models for the satisfaction of the internal model principle.
- Research on the cerebellum has implications for robotics, particularly in developing compliant, energy-efficient robots that remain robust to disturbances through their use of reflexes and cerebellar-like computations.

This paper is an extended version of the conference paper [19]. The present version places greater emphasis on the disturbance rejection aspect of cerebellar function, while [19] considered regulator theory in general. Specific differences between the two papers are as follows. "Experimental Evidence" is new. It reviews a number of distinct biological behaviors and experiments that are amenable to be interpreted under a common rubric of disturbance rejection. "Disturbance Rejection" provides an alternative presentation of the subject of disturbance rejection compared to the treatment in [19]. Whereas in [19] we adopted the standard control theoretic setup for disturbance rejection for LTI systems, without specific motivations for neuroscience problems, here we take more care to discuss the framework of disturbance rejection in a neuroscience context, thereby targeting readers who would not already have studied regulator theory and/or are not control theorists. Next, we include a discussion in "Disturbance Rejection" on how feedforward, reflex control inputs may be operated in tandem with internal models to perform disturbance rejection. Finally, we provide an expanded discussion on our visuomotor adaptation model in "Implications for Robotics", providing more details and clarifications on how these models function.

The paper is targeted at two potential groups of readers. First, we target control theorists who are interested to develop new control theory inspired by neuroscience. The experimental evidence section provides intriguing scenarios where a control theorist can ask: what makes such behaviors mathematically possible? Second, the article is addressed to neuroscientists who are interested in how a control theorist views the question of cerebellar function. The point of view expressed here is driven by mathematical possibilities, based on the available measurement structure of the cerebellum. If we are lucky, the mathematical possibilities will be limited, as in the case of the internal model principle, making the work of model building easier.

Cerebellum

The locus of internal models in the brain is believed to be the *cerebellum* [4, 20–27]. The cerebellum is a major brain region positioned at the back of the head, partly covered by the *cerebral cortex*, and itself covering the *brainstem*. Nobel prize winner John Eccles and his co-authors laid out the *microcircuit* of the cerebellum by 1967 [28]. Their work showed that the cerebellum contains relatively few neuron types, and that it has a laminated structure with a repeating architectural pattern pervading each functional *module*. Each module has only two input pathways and a single output pathway [29].

The first of two input pathways to the cerebellum is via the *mossy fiber* (MF) inputs. The MFs carry a rich flow of information from sensory inputs as well as the output of the cerebellum itself. Mossy fiber outputs are received by tens of billions of *granule cells*, the most common cell type of the brain. The axons of the granule cells form *parallel fibers*, which connect with the dendrites of the principal neuron type of the cerebellum, the *Purkinje cells* (PCs). Each PC receives synaptic connections from as many as 200,000 parallel fibers, resulting in a massive fan-in of information. The second input pathway to the cerebellum is via the *climbing fibers*, which are the axons of cells from the part of the brainstem called the *inferior olive*. The climbing fiber input carries a sensory error signal, and each climbing fiber forms a powerful connection with a single PC. Climbing fibers are capable to modify the strength of the synapse between parallel fiber inputs onto the PCs. The PC axons project to the *deep cerebellar nuclei* and the *vestibular nuclei*, forming the only output pathway from the cerebellum.

Notable features of the anatomical structure from a control perspective are:

(i) The cerebellum has a purely feedforward structure. Information flows from the MF inputs to granule cells and then via the parallel fibers to the PCs. The

PCs send their outputs to the deep cerebellar nuclei and vestibular nuclei.

(ii) Each functional module of the cerebellum is identical to the others and performs the same neural computation. The only distinction between modules is in terms of the input and output connections to other regions of the brain.

(iii) Each functional module of the cerebellum processes its own sensory error signal received via the climbing fiber inputs from a circumscribed region of the inferior olive. Each module sends its output to a circumscribed region in the cerebellar nuclei or vestibular nuclei.

(iv) The adaptive capability of the cerebellum is provided by the climbing fiber input which changes the strength of the synapse between the parallel fibers and the PCs.

(v) Mossy fibers projecting to a similar region of the cerebellar cortex encode similar information.

(vi) Each of the deep cerebellar nuclei and the vestibular nuclei has a projection to the MF inputs of the cerebellum. This projection is termed the *nucleo-cortical pathway* and is regarded to provide an *efference copy* of the motor command issued by the cerebellum [16, 17].

Structural Model

The features we have highlighted suggest a *structural model* associated with a single cerebellar module. This model does not reveal function but accords with cerebellar structure at a systems level:

$$\dot{x} = Ax + Bu + Ed_1 \tag{1a}$$

$$e = Cx + Dd_2 \tag{1b}$$

$$\dot{w}_1 = F_1 w_1 + G_1 u_{\mathrm{mf},1} \tag{1c}$$

$$\vdots$$

$$\dot{w}_k = F_k w_k + G_k u_{\mathrm{mf},k} \tag{1d}$$

$$\dot{w}_{k+1} = F_{k+1} w_{k+1} + G_{k+1} u_{\mathrm{im}} \tag{1e}$$

$$\hat{w} = (w_1, \ldots, w_{k+1}) \tag{1f}$$

$$\dot{\hat{\psi}} = \gamma e \hat{w} \tag{1g}$$

$$u_{\mathrm{im}} = \hat{\psi}^{\mathsf{T}} \hat{w} \tag{1h}$$

$$u = u_s + u_{\mathrm{im}}\,. \tag{1i}$$

Equation (1a) represents the open-loop system under regulation by the cerebellum: *horizontal eye position*, *eye velocity*, *hand position*, *hand grip force*, *gait*, *stance*, and so forth. This plant model is presented as a linear system for simplicity, but the cerebellum also regulates nonlinear plants such as the limbs. See "Nonlinear Models" where we discuss how nonlinear models can be incorporated. The signal $e \in \mathbb{R}$ is an error that the cerebellum is tasked with asymptotically driving to zero. Identifying the error signal associated with each cerebellar module is one of the central tasks of experimental neuroscience research on the cerebellum.

Signal $d_1 \in \mathbb{R}$ is a persistent exogenous disturbance entering at the plant input. Signal $d_2 \in \mathbb{R}$ is a persistent exogenous disturbance or reference signal entering at the error measurement. The term "persistent" in control theory means a signal sustained forever. The motivation for studying such disturbance signals is that it allows one to carry out a stability analysis without concern for the termination of the disturbance, thus simplifying the analysis. In practice, especially in neuroscience applications, one must allow for *episodic* disturbance rejection of signals that may be sustained over seconds or minutes while a particular motor task is being performed. For example, a "persistent" disturbance can be the rhythmic swaying of a subway train under one's feet during a 15 minute ride, or it can be a step reference signal that must be tracked for 2 s as one holds the gaze on an eccentric visual target. In these more realistic cases, the theoretical stability guarantees obtained under the "persistency" assumption remain valid. Finally, the term "persistent" must be contrasted with "transient disturbances", which are brief, typically impulsive disturbances that are either rejected through reflexes or through the inherent robustness of a closed-loop system. Internal models are not designed to handle transient disturbances. In summary, the term "persistent" refers to a class of disturbances that is ideally rejected using an internal model. The assumption that they persist forever is a convenient abstraction for the purposes of mathematical analysis.

Distinct MF input signals are $u_{\mathrm{mf},1}, \ldots, u_{\mathrm{mf},k}$ and u_{im}, which arrive by way of the filters (1c)–(1e) with corresponding filter states $w_1, \ldots, w_{k+1}$. We assume each F_i, $i = 1, \ldots, k+1$ is Hurwitz. These filters are in analogy with the lead-lag filters utilized in [13] to model the granular layer, but we allow a more general interpretation here. The filter (1e) is particularly important as it models the nucleo-cortical pathway. Namely, u_{im}, the output from the PC's of the cerebellum, is sent back as a mossy fiber input.

The Eq. (1g) is the standard gradient adaptation law to model the modifiable synapses between parallel fibers and PCs. The structural model is modular in the sense that other parameter adaptation laws may be considered to capture

synaptic plasticity (for instance to address robustness [30]). Several models of synaptic plasticity have been proposed [31, 32, 33, Ch. 5]. These models may also be incorporated as parameter adaptation laws. For example, a modified gradient law inspired by the *Use it or Lose It Principle* of synaptic plasticity [34] has been developed in [35, 36].

The signal e in (1g) is supplied by the climbing fiber input to the cerebellum. Parameter $\gamma > 0$ is the adaptation rate. The output of the cerebellum is u_{im}, and the overall motor command is u. It includes u_s for closed-loop stability, if needed. The motor command may also contain other feedforward or *reflex* signals. These can be included on a case by case basis, depending on which module of the cerebellum is being studied. Some examples are given in the text below. A control theorist will recognize the structural model to have the general form of an *adaptive observer* [11, 12].

Nonlinear Models

This paper has focused on linear time-invariant plant models for the sole reason that in our past work on the oculomotor system and visuomotor adaptation, linear models sufficed to capture the phenomena of interest. To further develop a framework for cerebellar function based on disturbance rejection, it is necessary to consider nonlinear plant models, nonlinear observers, and nonlinear internal models. Two areas where this extension is immediately required are visuomotor adaptation and adaptation of central pattern generators. In visuomotor adaptation nonlinear saturation phenomena are clearly evident in so-called *error clamp* experiments [37, 38]. Second, it is known that training of nonlinear oscillators and central pattern generators are subject to the influence of the cerebellum [39, 40]. See also [41] for related work on nonlinear oscillators modeled as adaptive observers.

On the control theory side, nonlinear regulator theory has been under development for the last 30 years [42–46]. These developments split into several separate research threads. First, there are many sophisticated nonlinear internal model designs available, with a brief list being [46–48]. Second, adaptive control has been significantly extended to include nonlinearly parametrized models [49–52]. Third, nonlinear adaptive observers (or forward models) have been developed in [12, 53–57].

Experimental Evidence

The structural model does not endow the cerebellum with any particular function except that of filtering MF inputs along with parameter adaptation. Our hypothesis is that the primary function of the cerebellum is disturbance rejection of exogenous disturbance and reference signals. We consider experimental evidence that we believe supports this hypothesis.

Gaze Holding

It is well known that a suitably accurate model of the oculomotor plant takes the form of a stable first- or second-order differential equation [58, 59]. This means it has no inherent capability to hold the gaze at eccentric positions, since this behavior involves tracking a step signal. The oculomotor system also has no direct measurement of eye position, since it has been shown that proprioception plays an insignificant role in eye movement [60–62]. To satisfy the internal model principle, the gaze holding system would require a pure integrator corresponding to a pole at $s = 0$ in the control loop to achieve step tracking with zero steady-state error. In early writings, it was thought that this integrator function was provided by the *brainstem neural integrator* (see the discussion in [63]). But the neural integrator is known to be leaky [58]. It is now more fully understood that the cerebellum is needed to complete the gaze holding function by supplying a top-up signal [63]. Our hypothesis is that the cerebellum contains an internal model for gazing hold that is capable to generate step signals. By estimating a step signal, the cerebellum provides for asymptotic rejection of the step reference signal arising in the retinal error signal, a positional error proportional to the angular distance from the fovea to the target on the retina [64].

Smooth Pursuit Eye Movements

The human and primate smooth pursuit eye movement systems are capable to track sinusoidal reference signals within a certain frequency band with nearly perfect precision, despite more than a 100 ms delay in the retinal error signal [59, 65–70]. This capability is particularly evident for predicable targets [66], leading neuroscientists to describe it as a "prediction" mechanism [71–74]. However, pure prediction is a non-robust mathematical operation in closed-loop, raising questions about how it could be implemented by a biological system for a pursuit task. On the other hand, we know that, mathematically speaking, the smooth pursuit system would have to acquire an internal model capable to generate sinusoids of a particular frequency to satisfy the internal model principle; otherwise, perfect tracking with near-zero steady-state error based on sensory errors is mathematically impossible. The prediction capability of the smooth pursuit system has been posited to lie outside the cerebellum in [74]. Our hypothesis is that the main locus for the so-called prediction capability of the smooth pursuit system is the cerebellum. We believe this hypothesis may be reasonable given the preponderance of experimental evidence supporting that

the cerebellum is crucial for proper function of the smooth pursuit system [59, 75].

Constant Velocity Visual Target Tracking

The oculomotor system is capable to track constant velocity targets with high precision [59]. Since the oculomotor plant is stable, the internal model principle informs us that, mathematically speaking, the closed-loop system should have an internal model of an *exosystem* with two poles at $s = 0$. Constant velocity target tracking is often treated as a separate behavior than sinusoidal tracking (the latter system is thought to have a predictive mechanism, as we discussed above). From a control theory perspective, the two behaviors are almost identical. In one behavior the internal model reconstructs a sinusoid while in the other it reconstructs a ramp signal. In principle, the cerebellar computations would be nearly identical. Indeed, we hypothesize that both ramp tracking and sinusoidal tracking are performed by the flocculus [7]. The hypothesis is, however, premised on the assumption that both ramp tracking and sinusoidal tracking are driven by a positional retinal error signal. If sinusoidal tracking is instead driven by a velocity-based error, namely the *retinal slip velocity* then a more likely locus of sinusoidal tracking would be the nodulus/uvula. Our point here is that differences between sinusoidal and ramp tracking would appear to have more to do with the sensory error that drives those specific eye movement systems, which in turn informs which module of the cerebellum is involved, and less to do with differences in cerebellar computations, which are conceptually identical.

Vestibulo-Ocular Reflex (VOR)

The vestibulo-ocular reflex provides an intriguing example of the role of disturbance rejection in the cerebellum when the exogenous disturbance is picked up by one of the sensory organs and then directly applied as a feedforward signal, a *reflex*, to a part of the body [76–78]. *VOR cancellation* is an experiment in which a subject must visually fixate on a head-fixed target while the body is rotated involuntarily in a sinusoidally rotating chair [59]. The VOR sends a reflex signal directly to the oculomotor neurons of the eye to make the eyes move nearly instantaneously in the opposite direction to the head. The purpose of the reflex is to provide fast rejection of head movement disturbances so that visual perception of a stationary visual field remains unblurred [59, 79]. During VOR cancellation, it is observed experimentally that the cerebellum issues a top-up signal to cancel the reflex signal [75, 78, 80, 81]. Since the reflex signal is sinusoidal when the chair movement is sinusoidal, the cerebellum must build an internal model capable to generate sinusoids of matching frequency to the chair frequency.

The VOR example invites a debate on whether rejection of reflex signals should be regarded as disturbance rejection of an endogeous or exogenous signal since the reflex signal is a signal within the body. From the point of view of the work of the cerebellum, we would argue that the origin of the disturbance is less relevant than the fact that the reflex signal is inappropriate during VOR cancellation. It must be cancelled by the cerebellum to drive the retinal error to zero.

Manual Interception of Falling Objects

It has been shown experimentally that astronauts initiate movement too early in zero gravity, and it has been posited that the brain acquires an internal model of the motion of a target under the effect of gravity [82–84]. We take a moment to clarify a distinction between an internal model of the dynamics of an object and internal models associated with the internal model principle of control theory. The equation of motion of a mass falling under the effect of gravity (without air resistance) is

$$\ddot{x} = g\,, \tag{2}$$

where g is the gravitational acceleration. While it may be postulated that the brain acquires a model of this law, the internal model principle states something different: that the brain must acquire an internal model of a *signal*. In particular, for a mass starting from rest at a height of x_0, the height evolves as

$$x(t) = x_0 - \frac{1}{2}gt^2.$$

The model for this signal takes the form

$$\dot{\zeta}_1 = \zeta_2 \tag{3a}$$

$$\dot{\zeta}_2 = \zeta_3 \tag{3b}$$

$$\dot{\zeta}_3 = 0 \tag{3c}$$

$$x = \zeta_3\,, \tag{3d}$$

a linear time-invariant third-order model with three poles at zero. Certainly humans are capable of visually tracking an object in freefall from a distance. The internal model principle informs us that, mathematically speaking, an internal model of the form (3) must exist somewhere in the brain.

Returning to the example of manual interception in zero gravity, if the motion of the falling object occurs over a very short time period, then there is insufficient time for the cerebellum to build an internal model of the continuous target motion. Rather, the learning process may correspond more closely to *visuomotor adaptation* in which an impulsive

movement of the arm is trained over repetitive trials; a behavior more amenable to modeling by a discrete-time or difference equation model. The current understanding is that the cerebellum is involved in adapting the timing of such movements [85].

Finally, we note that cerebellar training of reflex responses takes place over a much longer time scale (hours and days) relative to the primary function of the cerebellum, which can be initiated within 10–100 ms with the arrival of sensory error signals. For instance, learning appropriate responses in zero gravity is observed to require several days of experience [82]. Studies of adaptation of reflex responses provide valuable insight on processes downstream from the cerebellum—processes that are disrupted when the cerebellum is damaged [75, 86].

Voluntary v.s. Involuntary Motion

It has been shown experimentally that the cerebellum is involved in self-motion perception [76, 85, 87, 88]. In particular, the *nodulus* and *uvula* (together called the NU) of the *vestibulo-cerebellum* are required to process sensory information from the vestibular organs: the *otoliths* and *semicircular canals* of the ears, which provide linear and angular acceleration measurements, respectively, of the head. If the nodulus and uvula are lesioned, then self-motion perception in humans is impaired. The subject's awareness of self-motion is likely to be a higher cognitive function relative to cerebellar function, which appears to be automatic or implicit. Thus, we may hypothesize that awareness of self-motion is another auxiliary downstream process arising out of a well-functioning disturbance rejection capability in the cerebellum [89].

An underpinning of self-motion perception is the ability to distinguish motion generated endogenously and exogenously (modulo the complications we discussed in "VOR, Smooth Pursuit, and Gaze Holding"). For instance, self-generated v.s. passive head rotation was studied in [77, 87]. These studies found neurons in the vestibular nuclei of rhesus monkeys that are responsive to head rotation but do not reliably encode head velocity arising from self-generated head movement. This finding is not inconsistent with a disturbance rejection role of the cerebellum (of course, it depends on the specific class of neurons from which recordings are taken).

Feedforward (non-error based) components of a motor command are available to the cerebellum to assist in isolating exogenous disturbance and reference signals that impinge on sensory errors. If motion is entirely generated by feedforward motor commands without additional exogenous disturbances (as in the case of self-generated head rotation), then a cerebellum that performs disturbance rejection will not need to be active. Consequently, cells that are affected by cerebellar output (such as the PVP cells in the Roy/Cullen study) may adjust their modulation in concert with a reduced role of the cerebellum. Without the *efference copy* of feedforward motor commands, exogenous and endogenous signals would be scrambled together, resulting in the cancellation of useful signals. We will try to clarify these mathematical points in "Disturbance Rejection".

As mentioned, the term *exogenous* does not strictly refer to a signal generated by activity outside the body. A sensory signal may arrive from the environment, yet be incurred through one's own actions. For example, while running through the park, I activate my optokinetic system to track a moving visual field of trees. This self-induced disturbance in my vision may be regarded as "exogenous" with respect to the optokinetic system. No meaningful information in the motor command to my legs can be interpreted in terms of errors experienced by the visual system. The distinction between endogenous and exogenous or involuntary and voluntary movement depends on an interpretation of the boundaries of a given motor system.

Posture Regulation and Unexpected Motion

It has been shown in [90] that the cerebellum is capable to detect unexpected self-motion during posture regulation tasks. The authors performed a study to investigate the response of cells in the *rostral fastigial nucleus*, the most medial of the deep cerebellar nuclei, in rhesus monkeys. Neurons in this area receive an output from the PCs of the cerebellum, and they project their signals to the vestibular nucleus and the spinal cord to regulate posture. It was found that these cells are responsive when the head is passively rotated sinusoidally relative to the body, but the same neurons are not active when the monkey performed active head rotations. The findings are analogous to those for voluntary v.s. involuntary motion.

The interpretation of the experimental results in [90] from the point of view of the internal model principle is that the cerebellum estimates the sinusoidal head movement under the passive condition because there is some residual sinusoidal component in the proprioceptive error signals (to be regulated by the cerebellum) that is not fully canceled by the reflexes. Instead, under active rotation of the head, the motor command to the head and the reflexes are sufficient to provide complete cancellation of disturbances appearing in the error signals associated with maintaining a stable head position with respect to the torso. In our view, the research in [90] works toward a full understanding, both experimentally and mathematically, of the relationship between specific disturbance signals being *estimated* by the cerebellum and the associated error signals being *regulated*.

Disturbance Rejection of Gravity

Many studies have been performed to show that the cerebellum builds an internal model of gravity [91–93] in order that its contribution to certain reflexes may be removed.

The *otolith-ocular reflex* in humans is a reflex that stabilizes eye position relative to the visual surround. The reflex is elicited either during translational motion of the head or during angular motion that involves dynamic reorientation of the head relative to gravity. In order for the reflex to operate properly, it is necessary for the gravitation disturbance to be removed or cancelled from the reflex signal. The motivation for this computation by the brain is that gravity has no effect on the quality of visual perception, whereas linear displacement of the head does. For example, if the head movement is lateral, then the eye movement must remain horizontal for clear vision. Similarly, forward head movement requires that the eyes remain horizontal.

The difficulty with estimating gravity is that the otolith organs, which provide the drive for the otolith-ocular reflex, are unable to differentiate linear acceleration of the head from acceleration due to gravity. If the eye were to move according to the effect of the reflex only, and the reflex corresponds to the vector sum of gravity and linear acceleration in an inertial frame, then the eye would sustain torsional or vertical movements in the scenarios described above. A mechanism is needed to de-corrupt the reflex signal by removing the effect of gravity. It is known that the nodulus and uvula perform this function by performing an estimation of gravity, then subtracting it from the reflex signal in the overall motor command to the eyes [94].

In [91] subjects are rotated at a constant velocity about an earth-vertical axis. In steady-state, the semi-circular canals are unable to detect this motion since they only detect angular acceleration. Subjects are then rapidly decelerated to a stop, resulting in signals from the semi-circular canals that cue angular velocity in the opposite direction to the preceding rotation. Immediately after stopping, the subject is tilted by 90° to one of several orientations such as nose down. In this nose-down position, the otoliths pick up a constant linear acceleration due to gravity, while the semi-circular canals pick up a constant velocity rotation of the head about the body. It is observed that the eyes make compensatory movements in the dark that cannot be explained as a pure reflex response to the semi-circular canal and otolith signals. It is proposed that an estimation of gravity is made by the cerebellum (nodulus and uvula), and this estimate modifies the eye movements.

These exciting experiments can be a prime testing ground for the hypothesis that the cerebellum subserves the internal model principle: does the cerebellum estimate gravity so that gravity signals can be cancelled from reflex signals when the effect of gravity is inappropriate, with the ultimate aim to perform disturbance rejection in visual error signals?

Gait Regulation

In split-belt treadmill experiments, subjects must walk with belts moving at different speeds under each foot. Due to the repetitive and persistent nature of this disturbance, subjects are able to adapt the walking speed of each leg to maintain forward locomotion, while cerebellar patients are unable to perform this adaptation [39]. One may regard the differential in speed of the two belts as inducing a periodic disturbance which is detected through proprioceptive error signals in the feet. Alternatively (and equivalently), the speed of the two belts represents reference signals that must be tracked through leg movement. Reasoning through the lens of the internal model principle, given the essentially periodic nature of the disturbance that would arise, the internal model of the disturbance would likely be that of an oscillator of suitable frequency. The cerebellum would be invoked in this gait regulation task because pre-trained pattern generators in the spinal cord (which may be thought of as supplying reflex signals for walking) are unable on their own to maintain sensory (proprioceptive) error signals close to zero.

Adaptation in the Saccadic System

The saccadic eye movement system generates fast resets of eye position called *saccades*. This system is subject to a process of adaptation of the saccade size based on a measurement of the visual error between the fovea and the desired target immediately following the execution of a saccade [59, 95]. In *intersaccadic step* experiments, the target is shifted by a constant angle while the saccade is underway (there is no visual perception during a saccade because the movement is too fast), resulting in a predictable error between the final eye position and the (now displaced) target. From the point of view of the internal model principle, the cerebellum must reject a constant angular disturbance arising in the retinal error recorded at the end of the saccade. Our hypothesis is that the cerebellum contributes to the rejection of this disturbance by gradually adapting the saccade size using an internal model of a constant disturbance. The saccadic system does not appear to be capable of rejecting more complex time-varying disturbances [96]. This is an example of a motor system regulated by the cerebellum in which the class of disturbance signals which can be reconstructed appears to be extremely limited, in contrast with the slow-eye movement systems that can track steps, ramps, and sinusoids.

Rejection of Tail Movement During Fish Pursuit

Disturbance rejection by the cerebellum appears early in its evolutionary development. Cerebellum-like structures in fish have been shown experimentally to perform disturbance rejection [97–100]. Weakly electric fish use active electrolocation to nagivate and to find prey in the dark. The fish possess electric organs in the tail that emit weak electric fields, and electroreceptors along the body detect changes in this electric field. However, the electrosensory measurements are corrupted by the fish's own tail movement. Recordings from the output of the fish's cerebellum-like structure show that the fish is capable to reject the disturbance induced by tail movement to obtain a more accurate signal representing a prey object's position.

Disturbance Rejection

Our working hypothesis that the primary function of the cerebellum is disturbance rejection brings into view the subject of *regulator theory* [5]. In this section, we look at a representative *regulator design* to solve the disturbance rejection problem. This design is simple, and we suppress many details and extensions available in the control theory literature. Our mandate is a basic mathematical understanding of what the cerebellum may be doing, followed by a comparison with the structural model. The design utilizes *adaptive internal models*, for which many designs are now available in the literature [46].

Consider the open-loop system

$$\dot{x}(t) = Ax(t) + B(u(t) + d(t)) \tag{4a}$$

$$e(t) = Cx(t)\,. \tag{4b}$$

The first equation models the *plant* or open-loop system. Here it is represented as a linear system, but it can also be a nonlinear system; see "Nonlinear Models". The vector $x(t) \in \mathbb{R}^n$ is the *state*; $u(t) \in \mathbb{R}$ is the *control input* (or *motor command*); $e(t) \in \mathbb{R}$ is the *error* to be regulated; and $d(t) \in \mathbb{R}$ is a persistent, exogenous *disturbance* signal entering the plant at the control input. We can also include a second disturbance by writing

$$e(t) = Cx(t) + Dd_2(t)\,,$$

where $d_2(t)$ is a disturbance signal entering directly into the error signal. We omit this second disturbance primarily to keep the discussion simple.

The *disturbance rejection problem* is to find a (possibly nonlinear) *regulator*

$$\dot{x}_r(t) = f(x_r(t), x(t), e(t)) \tag{5a}$$

$$u(t) = h(x_r(t), x(t), e(t))\,, \tag{5b}$$

to make the error go to zero asymptotically, $e(t) \longrightarrow 0$, in the closed-loop system. The regulator has its own state $x_r(t) \in \mathbb{R}^p$, and it may receive a measurement of the plant state $x(t)$ and/or a measurement of the error $e(t)$. The design may be extended to include feedforward signals such as reflex signals, such as in (1i). Also, it is implicitly understood that the regulator can make use of the motor command $u(t)$ itself in its computations.

Next, we consider a representative *adaptive internal model* design, taken from [46]:

$$\dot{w}_0(t) = Fw_0(t) + FNx(t) \tag{6a}$$

$$\dot{w}_1(t) = Fw_1(t) - NAx(t) \tag{6b}$$

$$\dot{w}_2(t) = Fw_2(t) - NBu(t) \tag{6c}$$

$$\hat{w}(t) = w_0(t) + Nx(t) + w_1(t) + w_2(t) \tag{6d}$$

$$\dot{\hat{\psi}}(t) = \gamma(B^{\intercal}Px(t))\hat{w}(t) \tag{6e}$$

$$u_{\text{im}}(t) = -\hat{\psi}^{\intercal}(t)\hat{w}(t) \tag{6f}$$

$$u_s(t) = Kx(t) \tag{6g}$$

$$u(t) = u_s(t) + u_{\text{im}}(t)\,. \tag{6h}$$

It consists of three stable filters (6a)–(6c), with states $w_0(t), w_1(t), w_2(t) \in \mathbb{R}^q$, respectively, where it has been assumed that the matrix F is Hurwitz. These filters process three distinct input signals: $x(t)$, $Ax(t)$, and $Bu(t)$ (to be interpreted as the mossy fiber inputs to the cerebellum). The filter states are combined in (6d) to form the signal $\hat{w}$, which is the *regressor* for the parameter adaptation law (6e). The learning rate in the adaptation law is $\gamma > 0$. The component u_{im} is the output of the adaptive internal model (to be interpreted as the Purkinje cell output of the cerebellum). The component u_s is for closed-loop stability, with the gain K such that $A + BK$ is Hurwitz.

The term $(B^{\intercal}Px)$ in (6e) arises because we are presenting a design based on the measurement of the state x. This signal may be interpreted as a proxy for an error signal (modeling the climbing fiber input to the cerebellum). It renders the transfer function of the linear system to be *strictly positive real*, a property we exploited in our modeling work with the optokinetic system [10]. Precisely, $P \in \mathbb{R}^{n\times n}$ is the symmetric, positive definite solution of the Lyapunov equation $(A + BK)^{\intercal}P + P(A + BK) = -Q$, with $Q \in \mathbb{R}^{n\times n}$ symmetric and positive definite.

There are several constraints on the parameters of the adaptive internal model. We have already mentioned that

F is Hurwitz. Also, (F, G) must be a controllable pair. The latter is a commonsense requirement to ensure that the adaptive internal model does not lose information about the disturbance $d(t)$ that it is intended to estimate. The parameter N satisfies a constraint $NB = G$. This algebraic constraint may be interpreted in terms of structural information about how the plant is actuated; namely how the control input affects the plant. Such constraints on F, G, and N would have to be achieved at the neuronal level by biological processes that can match filter time constants and hold parameter values over many hundreds of millions of neurons in aggregate.

In this particular design, the plant parameters (A, B) are required to be available in the signals Ax and Bu. This assumption would be acceptable in a biological context if estimated signals $\hat{A}(t)\hat{x}(t)$ and $\hat{B}(t)u(t)$ were provided to the adaptive internal model by another adaptive brain process, such as a forward model or observer of the plant.

We now come to the important question of how the adaptive internal model is capable to estimate the disturbance $d(t)$. First, we look at the dynamics of $\hat{w}$. Using (6a)–(6d), we compute

$$\begin{aligned}\dot{\hat{w}}(t) &= Fw_0(t) + FNx(t) + N(Ax(t) + Bu(t) + Bd(t)) \\ &\quad + Fw_1(t) - NAx(t) + Fw_2(t) - NBu(t) \\ &= F\hat{w}(t) + Gd(t)\,.\end{aligned} \tag{7}$$

Equation (7) says that $\hat{w}$ will evolve according to a stable filter driven by the unknown disturbance $d(t)$, even though $d(t)$ is not directly available as a measurement. To further understand why this is useful, we consider that the role of the adaptive internal model will be to estimate disturbances that belong to a certain class of signals, organized according to their frequency content. For example, step, ramp, and single-frequency sinusoids have the property that they include at most one frequency component. Such signals can be modeled by a linear *exosystem*. The exosystem is a fictitious, mathematical construct that allows one to model disturbance signals in the form of differential equations. In other words, the exosystem does not physically exist, but it provides a template for what the adaptive internal model needs to do to estimate a signal. A useful parametrization of the exosystem takes the following form:

$$\dot{w}(t) = Fw(t) + Gd(t) \tag{8}$$

$$d(t) = \psi^{\mathsf{T}} w\,. \tag{9}$$

This exosystem uses the same parameters (F, G) as were implemented in the adaptive internal model (6). The only unknown parameter is $\psi \in \mathbb{R}^q$, and its value determines the frequency content of $d(t)$ [46]. We can see this by substituting the expression for $d(t)$ in (9) into (8):

$$\dot{w}(t) = (F + G\psi^{\mathsf{T}})w(t) =: Sw(t)\,.$$

The eigenvalues of S, fixed by the free parameter ψ, determine the class of signals that can be modeled by the exosystem in terms of their frequency content. In summary, parameters (F, G) are fixed by the design of the adaptive internal model, while $w(0)$ and ψ are the unknown quantities that precisely determine the signal $d(t)$. When we compare (8) with (7), we can understand that $\hat{w}$ is an estimate of w, $\hat{\psi}$ is an estimate of ψ, and u_{im} is an estimate of $d(t)$.

The fact that this regulator design meets the requirements of the internal model principle can be verified as follows. Consider the filter equation (6c) and suppose $\hat{\psi} = \psi$, the steady-state condition for the parameters to converge to their correct values. Substituting u into (6c), we have

$$\begin{aligned}\dot{w}_2 &= Fw_2 - NB(u_s + u_{\text{im}}) \\ &= Sw_2 + G\eta_2\,,\end{aligned}$$

where $\eta_2 = \psi(w_0 + Nx + w_1) - u_s$. We notice that if the disturbance rejection problem is solved, then in steady-state, the signal $\eta_2(t)$ is zero. Therefore, in steady-state the filter dynamics are:

$$\dot{w}_2 = Sw_2\,.$$

Again, the eigenvalues of S (equivalently the poles of the exosystem) determine the signals that can be generated by the exosystem, and the regulator now embeds a subsystem with the same signal generation capability. Mathematically, the regulator contains an internal model of the disturbance.

A final issue to address is how feedforward or reflex control inputs can be handled in the adaptive internal model. The relevance of this issue is that the cerebellum is involved in maintaining correct reflex responses [59, 86, 101]. To handle reflexes, the input (6h) is modified as

$$u_r(t) = -\hat{\alpha}_r^{\mathsf{T}} y_r(t) \tag{10a}$$

$$u(t) = u_r(t) + u_s(t) + u_{\text{im}}(t)\,, \tag{10b}$$

where $u_r(t) \in \mathbb{R}$ is the feedforward (reflex) input, $y_r \in \mathbb{R}^p$ represents sensory measurements, and $\hat{\alpha}_r \in \mathbb{R}^p$ are called *reflex gains* [86]. The parameters $\hat{\alpha}_r$ (here depicted as constant) are adjusted in a process called *long-term adaptation*, a process not explicitly modeled in this paper but the subject of our forthcoming work. The purpose of the reflexes is to instantaneously cancel measurable components of the disturbance. As such, we can consider the disturbance being split into two components

$$d(t) = d_1(t) + d_2(t)\,,$$

where $d_2(t)$ represents the part of the disturbance that is not measured by sensory measurements. If the reflex gains are

properly adapted, then the reflex completely or approximately cancels the other disturbance component:

$$u_r(t) = -d_1(t)\,.$$

There are two ways to handle this situation in terms of the adaptive internal model design. The first approach is to continue using the design (6) but with a modified input (10). Then $\hat{w}$ continues to evolve according to (7), therefore providing a filtered estimate of $d(t)$. But we only require a model of $d_2(t)$. This issue is resolved using properties of exosystems [46]. Namely, there exists a parameter $\psi_2 \in \mathbb{R}^q$ such that

$$d_2(t) = \psi_2^{\mathsf{T}} w(t)\,, \tag{11}$$

where $w(t) \in \mathbb{R}^q$ is the state of the exosystem (8). To avoid notational confusion, we can rewrite the parameter adaptation law (6e) and the output of the adaptive internal model (6f) as

$$\begin{aligned}\dot{\hat{\psi}}_2(t) &= \gamma(B^{\mathsf{T}} P x(t))\hat{w}(t)\\ u_{\mathrm{im}}(t) &= -\hat{\psi}_2^{\mathsf{T}}(t)\hat{w}(t)\,.\end{aligned}$$

We understand that $\hat{w}(t)$ remains an estimate of $w(t)$, whereas $\hat{\psi}_2(t)$ is an estimate of ψ_2 and not ψ. The role of u_{im} is to cancel the *residual disturbance* $d_2(t)$, which is not instantaneously cancelled by the reflexes. We call this design a *centralized design* because all reflex inputs must be provided to the adaptive internal model.

An alternative approach is to first cancel d_1 and u_r in the open-loop plant model (4a) to obtain obtained

$$\begin{aligned}\dot{x}(t) &= Ax(t) + B(u_s(t) + u_{\mathrm{im}}(t)) + Bd_2(t)\\ e(t) &= Cx(t)\,.\end{aligned}$$

This model suggests a modified adaptive internal model design:

$$\begin{aligned}\dot{w}_0(t) &= Fw_0(t) + FNx(t)\\ \dot{w}_1(t) &= Fw_1(t) - NAx(t)\\ \dot{w}_2(t) &= Fw_2(t) - NB(u_s(t) + u_{\mathrm{im}}(t))\\ \hat{w}(t) &= w_0(t) + Nx(t) + w_1(t) + w_2(t)\\ \dot{\hat{\psi}}(t) &= \gamma(B^{\mathsf{T}} P x(t))\hat{w}(t)\\ u_{\mathrm{im}}(t) &= -\hat{\psi}^{\mathsf{T}}(t)\hat{w}(t)\\ u_s(t) &= Kx(t)\\ u_r(t) &= -\hat{\alpha}_r^{\mathsf{T}} y_r(t)\\ u(t) &= u_r(t) + u_s(t) + u_{\mathrm{im}}(t)\,.\end{aligned}$$

We call this a *decentralized design* in the sense that the adaptive internal model does not receive a measurement of the reflex input u_r.

We summarize the main points of this section of the paper by comparing (6) with (1). There are three important points:

(i) The filter (6c), which fulfills the requirements of the internal model principle, corresponds to the nucleocortical pathway in (1e).

(ii) The model (6) bundles together filter inputs Nx, Ax, and Bu in (6a)–(6c) based on prior knowledge of the plant parameters. However, these filter inputs need not be aggregated in this way. Mathematically speaking, states or other sensory inputs may arrive as filter inputs according to a number of patterns or combinations, potentially depending on the structure of the open-loop system. This mathematical flexibility, in turn, may imply that an "unpacking" of MF inputs to the cerebellum is necessary to determine their constituent components, making the modeling problem more challenging.

(iii) The model (6) requires that all the filters (6a)–(6c) have synchronized to utilize the same filter time constants, i.e. $F_i = F_j$. Since the filters (1c)–(1e) or (6a)–(6c) are nominally intended to model the granular layer of the cerebellum, this raises the question of whether the granular layer is capable of some form of dynamic synchronization.

We have identified intriguing analogies between cerebellar structure and internal model designs for disturbance rejection from a regulator theory. But the comparison remains abstract. The *oculomotor system*, discussed in the next section, provides more concrete evidence that such analogies can be fruitful toward model building.

Oculomotor System

The *oculomotor system* comprises several eye movement systems: the *vestibulo-ocular reflex* (VOR), the *optokinetic system* (OKS), the *gaze fixation system*, the *smooth pursuit system*, the *vergence system*, and the *saccadic system*. The oculomotor system provides a good starting point for studying the cerebellum because it has a very simple plant (the eyeball), and it is believed to provide the blueprint for all other motor systems [59].

VOR, Smooth Pursuit, and Gaze Holding

In [6, 7] (see also [102]) we presented a model of the VOR, smooth pursuit, and gaze holding for the horizontal motion of one eye, by applying an adaptive internal model design from [47]. Let $x(t) \in \mathbb{R}$ be the horizontal eye angle with respect to the head. Let $x_h(t)$ be the horizontal head angle and $r(t)$ is the horizontal angular position of a target, both with respect to an inertial frame. The model is:

$$\dot{x}(t) = -K_x x(t) + u(t) \tag{12a}$$

$$\dot{\hat{x}}(t) = -K_x \hat{x}(t) + u(t) \tag{12b}$$

$$\dot{w}_1(t) = Fw_1(t) + Gu_s(t) \tag{12c}$$

$$\dot{w}_2(t) = Fw_2(t) + Gu_{\text{im}}(t) \tag{12d}$$

$$\hat{w}(t) = w_1(t) + w_2(t) \tag{12e}$$

$$\dot{\hat{\psi}}(t) = \gamma e(t)\hat{w}(t) \tag{12f}$$

$$e(t) = r(t) - x(t) - x_h(t) \tag{12g}$$

$$u_b(t) = \alpha_{\text{X}}\hat{x}(t) - \alpha_{\text{VOR}}\dot{x}_h(t) \tag{12h}$$

$$u_s(t) = Ke(t) \tag{12i}$$

$$u_{\text{im}}(t) = \hat{\psi}^{\text{T}}(t)\hat{w}(t) \tag{12j}$$

$$u(t) = u_b(t) + u_s(t) + u_{\text{im}}(t)\,. \tag{12k}$$

Equation (12a) is the first-order model of the oculomotor plant [103]. Equation (12g) is the *retinal error*, the difference between the target angle $r(t)$ and the gaze angle $x(t) + x_h(t)$. It is this error that the cerebellum is tasked with driving asymptotically to zero. Equation (12b) models the brainstem *neural integrator* [104] which acts as an observer to provide an estimate $\hat{x}$ of eye position [105]. Equations (12c)–(12f) comprise the adaptive internal model in the cerebellum. The motor command $u(t)$ has a component u_b corresponding to a brainstem-only pathway for pure feedforward (reflex) signals, a component u_s to improve closed-loop stability, and u_{im}, the cerebellar output from the PCs.

The model can be compared to the known neural circuit associated with these eye movement systems [106]. The error signal (12g) is transmitted from the *visual cortex* to the inferior olive (IO), where it is relayed to appropriate climbing fiber inputs (CFs) of the cerebellum, specifically, the module called the *floccular complex*. This is the signal e appearing in (12f). The cerebellum also receives mossy fiber (MF) inputs from the *medial vestibular nuclei* (MVN) in the brainstem (B). These are the MF inputs in (12c)–(12d). The sole output of the cerebellum is u_{im}, transmitted via its Purkinje cells (PCs) to *floccular target neurons* (FTNs) in the MVN [107]. The MVN also receives a head velocity signal from the semicircular canals of the ear, signal $\dot{x}_h(t)$ in (12h), corresponding to the VOR. The parameter α_{VOR} is the *VOR gain*. The eye position signal $\alpha_{\text{X}}\hat{x}(t)$ corresponds to the projection from the brainstem *nucleus prepositus hypoglossi* (NPH) to the oculomotor neurons (MNs) which drive the eye. The output of the MVN is sent both to the neural integrator (NI) in the NPH and directly to the MNs of the oculomotor plant.

As we discussed in "Disturbance Rejection", the MF inputs in (12c)–(12d) may be bundled in a number of ways with a minor effect on overall behavior. For example, the two filters (12c)–(12d) could be combined into one, as was done in [108], for a more parsimonious model

$$\dot{\hat{w}} = F\hat{w} + G(u_s + u_{\text{im}}).$$

This modification affects the choice of parameters being adapted, but it does not affect overall model behavior. Alternatively one could write

$$\begin{aligned}\dot{w}_1 &= Fw_1 + FGe\\ \dot{w}_2 &= Fw_2 + G(u - u_b)\\ \hat{w} &= (w_1, w_2)\end{aligned}$$

The feedforward signals in u_b are now arriving as MF inputs to be subtracted from the overall motor command. This subtraction of feedforward signals is required so that their effect is not cancelled by the cerebellum (the cerebellum provides a top-up to the action of feedforward signals). Depending on the origin of the constituent components of the motor command u in the brain, such an explicit subtraction of certain MF inputs may arise, if not for the floccular complex, possibly in another cerebellar module. Such a situation would certainly cloud an understanding of the role of certain MF inputs to the cerebellum.

The model (12) recovers the standard lesion, behavioral, and neurological experiments associated with the VOR, gaze holding, and smooth pursuit; see [6, 7]. Here we discuss two important experiments that highlight the special capabilities of the cerebellum.

A first experiment called the *error clamp* explores the role of the error signal using a technique called *retinal stabilization* [109–111]. A monkey is trained to track a visual target moving horizontally at constant speed. After reaching steady-state, the error is optically clamped at zero using an experimental apparatus that centers the target image directly on the fovea. In experiments, it is observed that, despite zero error, the eye continues to track the target for some time after. Neuroscientists postulate so-called *extraretinal signals* drive the smooth pursuit system. Figure 1 depicts the error clamp with our model, showing on the left that the eye continues to track the target despite the measurement being clamped at $e \equiv 0$ during the time interval $t \in [5, 6]$. The right figure shows the (physical) error $r(t) - x(t)$. We see that some oscillations occur during tracking with the visual error clamped, showing that this open-loop operation is not robust. Nevertheless, the eye continues to track the target.

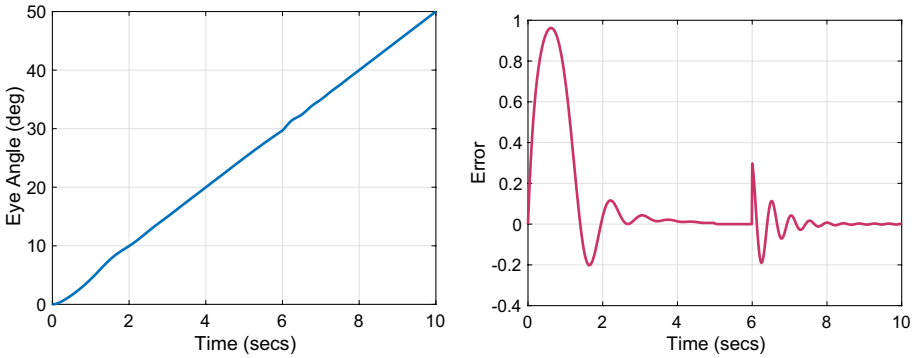

Fig. 1 Smooth pursuit with an error clamp during $t \in [5, 6]$ s. The eye angle x on the left and the error e on the right

In the second experiment called *target blanking*, a horizontally moving target is temporarily occluded, yet the eye continues to track the target [4, 112]; researchers have postulated the brain has an internal model of the motion of the target. Indeed, direct measurement of the appropriate PCs of the cerebellum shows that they remain active during the time that the target is occluded.

Let's consider the meaning of these experiments in terms of (12). In the first experiment, the error is clamped at zero, so we can set $e \equiv 0$ to obtain

$$\begin{aligned}\dot{w}_1(t) &= Fw_1(t)\\ \dot{w}_2(t) &= Fw_2(t) + Gu_{\text{im}}(t)\\ \hat{w}(t) &= w_1(t) + w_2(t)\,.\end{aligned}$$

Since F is Hurwitz, the first filter state $w_1(t)$ decays to zero. Then the second filter evolves (in steady-state) according to $\dot{w}_2 = (F + G\psi^{\intercal})w_2$, where $F + G\psi$ has two zero eigenvalues to model a ramp signal. In addition, we assume that $\hat{\psi}$ has converged to ψ. Clearly, w_2 provides the drive for continued pursuit during the error clamp. But this behavior is only ensured because of the nucleo-cortical pathway which provides the efference copy of u_{im}.

In the second experiment, there is no error signal while the target is occluded. It would certainly be paradoxical for the cerebellum to continue to supply (on its own) a drive for pursuit when there is no sensory error. Therefore, we must postulate that a higher brain center gates the activity of the nucleo-cortical pathway. When that gate is closed, the drive for pursuit is maintained. When the gate is open, the drive is disrupted.

In summary, when there is no error signal and/or the subject is not interested in an external stimulus, then the nucleo-cortical pathway may be disabled, resulting in the stable model

$$\begin{aligned}\dot{w}_1(t) &= Fw_1(t)\\ \dot{w}_2(t) &= Fw_2(t)\\ \hat{w}(t) &= w_1(t) + w_2(t)\,,\end{aligned}$$

in which all filter states gradually decay to a quiescent level of activity. However, when an error signal is temporarily dropped but the subject remains interested in the stimulus, then it is conceivable that the nucleo-cortical pathway is not disabled, at least for some period of time.

Optokinetic System

In the previous section we considered a model of a part of the cerebellum, the floccular complex (FC), involved in the regulation of the vestibulo-ocular reflex, smooth pursuit, and gazing hold eye movement systems. This section discusses a second functional module of the cerebellum, the nodulus and uvula (NU) which is responsible for regulating *the optokinetic system*.

The optokinetic system is an eye movement system to stabilize vision on a full-field moving visual surround. This eye movement system contrasts with the eye movement systems of the previous section whose goal is to stabilize an object on the fovea. How the optokinetic system interacts with the other eye movement systems is of great interest scientifically, but also theoretically from the perspective of control theory: can parallel adaptive internal models work collaboratively to regulate the same error? Or does the brain utilize a switching mechanism to switch from one adaptive internal model to the other, reminiscent of switched system architectures for adaptive control [113]? See [114] for a related interpretation.

Pioneering experimental work in the 1970s on the optokinetic system [115–118] lead to the discovery of the velocity storage mechanism (VSM), a behavior in which eye velocity is stored while following a constant velocity visual surround, even with intervening *saccades* (a fast reset of eye position) in a behavior called *nystagmus*. A striking feature of the VSM is that it partially meets the requirements of the internal model principle, in the sense that the longer the time constant of the VSM, the better the optokinetic system is able to track a step signal in velocity—as though evolution made a first attempt at architecting a neural internal model. Indeed, the velocity storage mechanism of the VOR

is known to prolong the time-constant of the head angular velocity signal from the semi-circular canals by a factor of 2–5 [115].

In [10] we proposed a model of the horizontal optokinetic system given by

$$\dot{x}_1(t) = x_2(t) \tag{13a}$$

$$\dot{x}_2(t) = \alpha_2(-x_2(t) - K_x x_1(t) + u(t)) \tag{13b}$$

$$e(t) = \dot{x}_w(t) - \dot{x}_h(t) - x_2(t) \tag{13c}$$

$$\dot{\hat{x}}(t) = -K_x \hat{x}(t) + u(t) \tag{13d}$$

$$\dot{v}(t) = -K_v v(t) + K_v e(t) \tag{13e}$$

$$\dot{w}_0(t) = F w_0(t) + FGe(t) \tag{13f}$$

$$\dot{w}_1(t) = F w_1(t) - Ge(t) \tag{13g}$$

$$\dot{w}_2(t) = F w_2(t) - G u_{\text{im}}(t) \tag{13h}$$

$$\dot{w}_3(t) = F w_3(t) - G\hat{x}(t) \tag{13i}$$

$$\dot{w}_4(t) = F w_4(t) - G\dot{x}_h(t) \tag{13j}$$

$$\dot{w}_5(t) = F w_5(t) - Gv(t) \tag{13k}$$

$$\hat{w}(t) = (w_0(t) + Ge(t), w_1(t), w_2(t), w_3(t), w_4(t), w_5(t)) \tag{13l}$$

$$\dot{\hat{\psi}}(t) = \gamma e(t)\hat{w}(t) \tag{13m}$$

$$u_{\text{im}}(t) = \hat{\psi}^{\intercal}(t)\hat{w}(t) \tag{13n}$$

$$u_b(t) = \alpha_{\text{x}}\hat{x}(t) - \alpha_{\text{VOR}}\dot{x}_h(t) + \alpha_{\text{OK}}e(t) + \alpha_{\text{v}}v(t) \tag{13o}$$

$$u(t) = u_b(t) + u_{\text{im}}(t)\,. \tag{13p}$$

We utilized a second-order model of the oculomotor plant in (13a)–(13b), with $x_1(t)$ the horizontal eye angle and $x_2(t)$ the eye angular velocity, because the optokinetic system stabilizes eye velocity, not eye position. The error signal $e(t)$ in (13c) to be regulated by the cerebellum is the *retinal slip velocity*, the difference between the horizontal angular velocity of the visual field $\dot{x}_w(t)$ and the gaze velocity $x_2(t) + \dot{x}_h(t)$. A non-zero $\dot{x}_w(t)$ is induced in experiments when a subject is seated inside a rotating optical drum. The brainstem neural integrator again appears in (13d). Equation (13e) is the *velocity storage integrator* of the optokinetic system, modeled as a leaky integrator with state $v(t)$ [115]. The motor command $u(t)$ is now regarded as an acceleration input to this second-order plant model; $\alpha_{\text{OK}}e(t)$ captures the drive provided by the *optokinetic reflex*, where α_{OK} is the called the *optokinetic gain*; the vestibulo-ocular reflex is modeled by $\alpha_{\text{VOR}}\dot{x}_h(t)$, as before. The term $\alpha_{\text{v}}v(t)$ captures the drive provided by the velocity storage integrator. Finally, we mention that there is no stabilizing feedback u_s in this model because the velocity dynamics of the oculomotor plant are already highly stable. The filters (13f)–(13k) correspond to the granular layer that filters the mossy fiber inputs.

In comparing this model to the structural model (1), we observe the additional filters (13i)–(13k) driven by feedforward signals $\hat{x}(t)$, $\dot{x}_h(t)$, and $v(t)$. Mathematically speaking, it can be shown that if these signals are not included as MF inputs, then they would be cancelled or rejected by the activity of the NU, as predicted by the model. Thus, a pattern we have already highlighted on the variable roles of certain MF inputs is reinforced again with this model: mathematically speaking, MF inputs may either appear because they are directly involved in disturbance estimation (such as e and u_{im}), or they may appear to avoid being cancelled by the cerebellum.

The model (13) is consistent with the neural circuit, and it recovers five standard behaviors of the optokinetic system: *optokinetic nystagmus* (OKN); *optokinetic after-nystagmus* (OKAN I); *OKAN suppression*; *OKN suppression*; and *OKAN II*. OKN is an eye movement in which the eye tracks the velocity of a (full-field) moving visual surround during the so-called *slow phase*, followed by a saccade to rapidly reset the eye position to zero in the *fast phase* [115, 116]. OKAN I is a behavior following OKN when the lights are turned off. During OKAN I nystagmus continues in the same direction as OKN, even though there is no visual stimulation [115, 119].

Figure 2 shows simulation results for OKN and OKAN I using our model, with the optokinetic drum rotating at a constant velocity of 60°/s for 60 s. The initial jump in slow phase eye velocity is attributable to the large retinal slip velocity at the onset of the experiment and the charging of the VSM. The non-zero steady-state error during OKN is observed because the NU internal model is “untrained". Once the lights are extinguished at $t = 60$s, visual signals are no longer present and the NU is effectively inactive, the signal e is unavailable, and $u_{\text{im}} = 0$ (based on gating the nucleo-cortical pathway). This causes the slow-phase eye velocity to rely on the dynamics from the VSM, which slowly dissipates its stored velocity, creating OKAN I.

If the subject is involved in repeated trials of the same experiment eliciting OKN and OKAN I, the NU internal model is “trained” over time. Consequently, the OKN steady-state slow-phase eye velocity increases [120, Fig 1]; the OKAN I time constant decreases [115, Fig 7]; and the

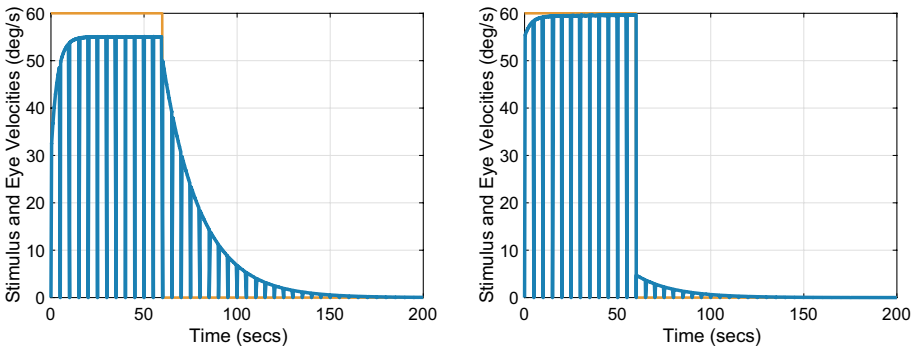

Fig. 2 Untrained (left) and trained (right) OKN and OKAN I

OKAN I duration decreases [118, Fig 2, 3]. These results are shown on the right of Fig. 2.

This section has demonstrated that a disturbance rejection interpretation of cerebellar function can be propitious to arrive at plausible models for one motor system: the oculomotor system. However, one may also utilize regulator theory to understand other adaptive behaviors that are best modeled as discrete, repetitive processes. Perhaps the most widely studied adaptive, discrete process is visuomotor adaptation, considered in the next section.

Visuomotor Adaptation

Visuomotor adaptation is a subconscious, "machine-like" brain process taking place over repetitive trials and elicited by a *visual error* closely following the execution of a movement. Visuomotor adaptation is intended to calibrate over a lifetime the mapping between what is seen and how to move. As a means to expose the underlying computations of this brain process, neuroscientists create experiments that artificially perturb what is seen by the subject during movement. Examples include saccades with an intersaccadic step of the target [121]; the *visuomotor rotation experiment* with fast arm reaches [122, 123]; and throwing darts while looking through prism glasses [124].

Visuomotor adaptation experiments consist of repetitive trials of a certain movement such as a saccade or arm reach. The trials are classified by type, and sequences of blocks of trials of specific types are utilized to elicit so-called dynamic behaviors of adaptation. A *baseline* (B) block familiarizes the subject with the experimental aparatus under unperturbed, normal conditions. A *learning* (L) block occurs after a baseline block when a perturbation or disturbance is introduced. A *washout* (W) block follows a learning block when the perturbation is removed. An *unlearning* (U) block follows a learning block when the perturbation changes in sign but not magnitute relative to the learning block. A *relearning* (R) block is a second learning block with the same perturbation. A *downscaling block* (D) is a second learning block in which the perturbation is set to a fraction of its value in the first learning block. A *no-visual-feedback* (N) block is a block of trials in which no visual feedback about the movement is presented to the subject. An *error clamp* (C) block is a block of trials when the visual error presented to the subject is clamped artificially to a value unrelated to the subject's movements. When blocks of trials are sequenced in a particular order and with a particular number of trials in each block, then several phenomena emerge in experiments:

- *Savings* is a behavior in which learning is sped up in the second learning block relative to the first one.
- *Reduced savings* is a behavior in which savings is reduced by inserting a washout block of trials after the unlearning block. After the washout block, relearning does not proceed as rapidly as in the savings experiment.
- *Anterograde interference* is a behavior in which a previously learned task reduces the rate of subsequent learning of a different (and usually opposite) task.
- *Rapid unlearning* is a behavior in which the rate of unlearning is faster than the rate of initial learning if the number of trials in the learning block is small.
- *Rapid downscaling* is a behavior in which the rate of learning in a secondary learning block is faster when the rotation is set to a fraction of its value in the initial learning block.
- *Spontaneous recovery* is a behavior observed during the washout block of a BLUW experiment in which the response partially "rebounds" to its value at the end of the learning block rather than converging monotonically to zero.

We used regulator theory to develop a model of visuomotor adaptation in [8, 9] with the goal to recover the six standard behaviors of visuomotor adaptation. The model was based on three assumptions. First, we focused on motor adaptation tasks involving one degree of freedom of movement; for instance, horizontal movement of the eye, hand angle relative to a reference angle in a horizontal plane, forward (coronal) inclination of the body relative to a vertical reference, the horizontal angle of a dart thrown by a subject, and so forth. Second, we assumed

the open-loop model is linear time-invariant. Third, we focused on constant disturbances, as currently there is a dearth of experiments with non-constant disturbances [96].

Let integer k be the trial number; $x(k)$ is the state of a single degree of freedom of the body at the end of the k-th trial; $d(k)$ is an additive disturbance in the measurement during the k-th trial; and $e(k)$ is the error between a visually reported position $y(k) = x(k) + d(k)$ observed by the subject at the end of the k-th trial (for example, a cursor on a computer screen representing the hand position) and a reference position $r(k)$. Our discrete-time model of visuomotor adaptation is:

$$x(k+1) = Ax(k) + Bu(k) \tag{14a}$$

$$e(k) = r(k) - x(k) - d(k) \tag{14b}$$

$$w_0(k+1) = Fw_0(k) + FGe(k) \tag{14c}$$

$$w_1(k+1) = Fw_1(k) - Ge(k) \tag{14d}$$

$$w_2(k+1) = Fw_2(k) - Gu(k) \tag{14e}$$

$$\hat{w}(k) = w_0(k) + Ge(k) + Aw_1(k) - Bw_2(k)) \tag{14f}$$

$$u(k) = Ke(k) + \psi\hat{w}(k)\,. \tag{14g}$$

The open-loop system model (14a) provides a high-level, abstract description of the quantitative change over successive trials of a single degree of freedom of the body. The term $Ax(k)$ models a retention or memory mechanism of the state in the previous trial. As before, we assume the filters (14c)–(14e) are stable; that is, F is Schur stable. We have not written a parameter adaptation law for any unknown parameters (although one may do so) since experiments show that the parameters vary extremely slowly; see [8]. The controller u has the same components as before: $u_s(k) = Ke(k)$ is to improve closed-loop stability, while $u_{\text{im}} = \psi\hat{w}(k)$ is the component to satisfy the internal model principle. We discuss the role of $\psi \in \mathbb{R}$ below.

To understand why the internal model (14c)–(14f) is suitable for disturbance rejection of the perturbation $d(k)$, we perform the same calculation as we did in (7), but now working in discrete-time. To facilitate this calculation, it is helpful to first derive an *error model*, which informs on the evolution of the error. Using (14), we obtain an error model

$$e(k+1) = Ae(k) - Bu(k) + (A-1)d(k)\,,$$

where we have assumed $d(k+1) = d(k)$ for a constant perturbation. Next we compute

$$\begin{aligned}\hat{w}(k+1) &= w_0(k+1) + Ge(k+1) + Aw_1(k+1) - Bw_2(k+1))\\ &= F\hat{w}(k) + G(A-1)d(k)\,.\end{aligned}$$

We observe that, irrespective of the choice of $u(k)$, $\hat{w}(k)$ evolves according to a stable filter driven by the unknown disturbance $(A-1)d(k)$, which is the *effective* disturbance arising in the error model. It is therefore possible to use $\hat{w}(k)$ toward cancellation of that disturbance using the input $u(k)$.

To appreciate that our model generates all the standard dynamic behaviors associated with visuomotor adaptation [122], we consider the behavior called *savings*. Figure 3 shows a simulation for a BLUR experiment to elicit savings. The parameter values are: $A = 0$, $B = 1$, $F = 0.8$, $G = 1 - F$, $\psi = 1$, and $K = 0.22$. The top left figure shows the disturbance value $d(k)$ as a function of k, and the top right figure shows $x(k)$. We see that in a first learning (L) block the disturbance is $d(k) = -30°$. In the brief unlearning (U) block, it is set to its opposite value $d(k) = +30°$. In the relearning (R) it is again $-30°$. The bottom figure shows $x(k)$ during the learning block superimposed with $x(k)$ during the relearning block. We see that relearning is faster than learning, demonstrating that savings have indeed occurred in the relearning block.

Visuomotor adaptation experiments analogous to the error clamp and target blanking experiments for the smooth pursuit system, discussed in "VOR, Smooth Pursuit, and Gaze Holding", have also been performed. These provide dramatic evidence of the brain's capability to enable or disable internal models. We highlight two interesting experiments. First, many experimental studies of the form BLN have been conducted on the effect of removing the visual error in an N block following a learning block [125–127]. The major finding is that during the N block, $x(k)$ slowly returns to a nominal reference position. Further, Figure 2 of [126] shows that the rate of decay is faster in a washout (W) block than a no-visual feedback (N) block.

As we already discussed for the oculomotor system, when there is no error measurement, we must remove the signal $e(k)$ from every filter input in (14). To disable the internal model, it is also necessary to disable the efference copy $u(k)$ in (14e). The resulting internal model will consist of filters that are all stable, and therefore $\hat{w}(k)$ will gradually return to a zero reference value. In summary, if we assume that visuomotor adaptation operates in a manner that is consistent with the oculomotor system, then gating the nucleo-cortical pathway may provide an explanation for how internal models can be enabled or disabled in visuomotor adaptation. Figure 4 shows the results for (14) for a BLN experiment using this method to disable the internal model during the N block. Despite the appeal of relating visuomotor adaptation experiments with slow-eye movement experiments through a common conceptual mechanism, there is no explicit experimental evidence to date supporting that the behavior observed in

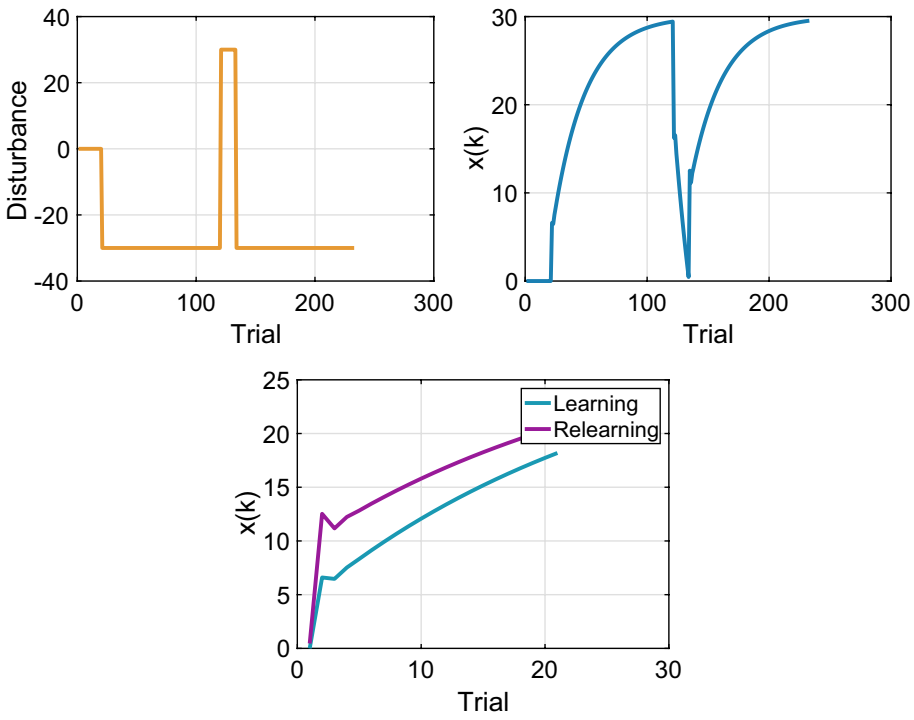

Fig. 3 Savings in a BLUR experiment. In the bottom figure $x(k)$ during the learning block is plotted in blue superimposed with a horizontally shifted version of $x(k)$ during the relearning block in purple. The purple curve is larger than the blue curve corresponding to faster learning in the relearning block

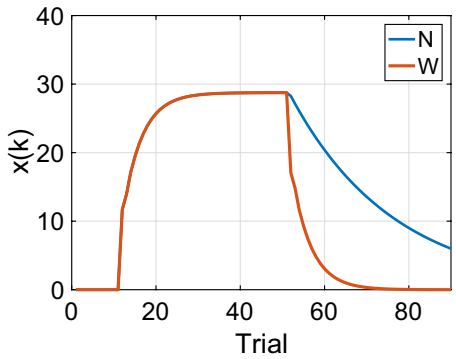

Fig. 4 BLN experiment v.s. BLW experiment

the N block is indeed driven by an internal model. Our main point is that, in mathematical terms, there exists a simple mechanism to explain how an internal model could be disabled by the brain when a visual error signal does not appear (within a specific time window following movement).

A second set of interesting experiments regarding the error clamp, with the form BLC, have been reported including [126, 128, 129]. In these experiments a subject makes fast arm reaches to a target on a computer screen while observing a cursor intended to represent the hand position at the end of a reach. A disturbance $d(k)$ is introduced during the learning blocks so that the observed cursor angle is $y(k) = x(k) + d(k)$. During error clamp blocks, the error observed by the subject is clamped at a constant value $e(k) \equiv \bar{e}$. Figure 2 of [129] reported results with various statistics on the error clamp value. These experiments further expose interesting on/off behavior of internal models associated with visuomotor adaptation. In a clamp (C) block with $e(k) \equiv -2.7$, it is observed that the hand angle remains close to its value at the end of the learning block. In a C block with $e(k) \equiv 0$, the hand angle returned to zero at a slow rate. Figure 5 shows the behavior of our model in a BLC(−2.7) experiment. We observe the hand angle remains close to 30°, its value at the end of the learning block, as reported in [129]. By comparison, the right figure shows a BLC(0) experiment. Now the hand angle slowly returns to zero.

The behavior in Fig. 5 is nothing like what a control theorist expects of an internal model. We expect that when $e(k)$ is clamped at zero, the behavior is as in the left of the figure, but when $e(k)$ is clamped at a non-zero value, the internal model is unstable. Instead, the experiments demonstrate that the human brain has made a "hedge" on the internal model principle: zero error signals induce a return to a quiescent state, while a persistent, small, non-zero error is necessary to keep the internal model active. We have used the parameter $0 < \Psi < 1$ to quantitatively characterize this hedge. However, we emphasize this modeling intervention need not represent the true physiological character of these experiments. We believe there are deeper meanings behind the curious phenomena reported in [129].

We summarize this section thus: current experimental evidence may well point to the idea that the reason for the special wiring of the cerebellum, particularly the

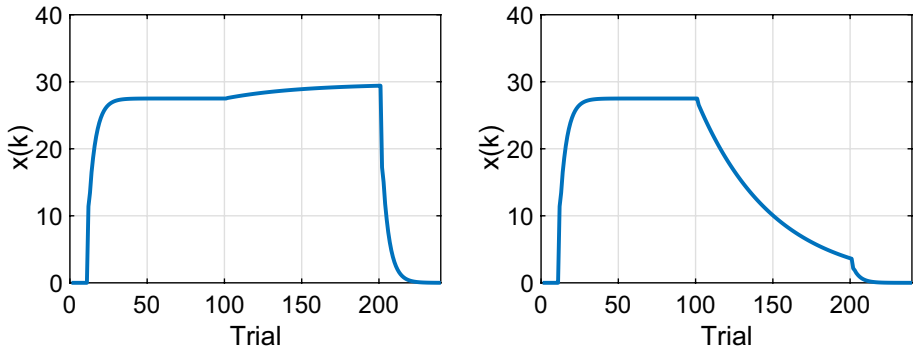

Fig. 5 BLC experiment, comparing C(−2.7) and C(0) blocks

nucleo-cortical pathway, is to implement the delicate operation of enabling and disabling internal models without inducing abrupt or unstable behavior in the subject.

Implications for Robotics

We have given evidence that there is value to study the cerebellum from the perspective of disturbance rejection and to utilize regulator theory and internal models of control theory to derive models of cerebellar function. We argue here that the study of the cerebellum using regulator theory has implications for robotics. We make our case using an example of a robot learning a new tool [20]. The discussion is informal, as the primary aim is to stimulate new ideas rather than to prove the correctness of fully developed algorithms, etc.

Consider a robot equipped with an arm and foveated, movable cameras resembling the functionality of the human eye. The robot is capable to perform rapid reaching movements with its arm using feedforward, pre-learned commands. The robot is tasked with performing such rapid movements while manipulating a new handheld tool - for example, a brush with a long handle to remove brambles from a dog. We pose the problem of training the robot to learn a new tool as a disturbance rejection problem. For simplicity, we consider one degree of freedom of movement, say the final horizontal angle of the robot's end effector at the end of a reach. We make the following assumptions:

Assumption 8.1

- N stationary targets are randomly positioned in the robot's visual field but sufficiently separated so that the robot is able to measure a distinct error between the arm (or the tool) end effector and any target. Let r_i denote the horizontal angular position of the ith target, where $i \in \{1, \dots, N\}$.
- Each target i has associated with it a feedforward (non-error-based) motor command denoted $u_{f,i}$ that was acquired through prior experience during nominal behavior (without using tools). We assume $u_{f,i}$ drives the robot end-effector directly to target position r_i with negligible error under nominal conditions.
- The visual field is partitioned into sectors called *adaptation fields*. Each adaptation field has associated to it an adaptive internal model. For simplicity and ease of discussion, we assume there is only one target within each adaptation field. Thus, we consider N adaptation fields and N internal models.
- Because it is highly expensive to process full-field visual information, the robot only records error measurements for one target at a time. Thus, the robot has the efficacy to select one target at the end of each reach, with respect to which it forms an error measurement $e(k)$. The index of the target that forms the error measurement at the end of the kth reach is denoted $m(k) \in \{1, \dots, N\}$.
- The robot has the efficacy to choose one target for the next reach. The index of the target for the $(k+1)$th reach is denoted $t(k) \in \{1, \dots, N\}$.

Let $x(k)$ represent the robot end-effector horizontal angle at the end of the kth reach, and $d(k) \equiv d$ is the constant angular offset introduced by the tool. The open-loop model is:

$$x(k+1) = u(k)$$
$$e(k) = r_{m(k)} - x(k) - d(k)\,.$$

The first equation says the robot is capable to move to any commanded horizontal angular position by using a motor command relying on data from the previous reach only. The second equation defines the visual error measured at the end of the kth reach, namely the difference between the angular displacement of the $m(k)$th target, $r_{m(k)}$, and the angular displacement of the end of the tool, $x(k) + d$.

Next, we define the update of the internal models. We assume that the trigger signal to update any internal model is its own error signal. In other words, index $m(k)$ determines which internal model is updated. The internal model update with index $m(k)$ is

$$w_{0,m}(k+1) = Fw_{0,m}(k) + FGe(k) \tag{15a}$$

$$w_{1,m}(k+1) = Fw_{1,m}(k) + G(u(k) - u_{f,m}) \tag{15b}$$

$$\hat{w}_m(k) = w_{0,m}(k) + Ge(k) + w_{1,m}(k)\,, \tag{15c}$$

where $m \equiv m(k)$. We are using a reduced set of filters compared to the previous internal model design (14) because $A = 0$. All other internal models, with index $i \in \{1, \dots, N\}$, $i \neq m(k)$, have an update of the form:

$$w_{0,i}(k+1) = F_n w_{0,i}(k) \tag{16a}$$

$$w_{1,i}(k+1) = F_n w_{1,i}(k) \tag{16b}$$

$$\hat{w}_i(k) = w_{0,i}(k,i) + w_{1,i}(k)\,. \tag{16c}$$

This second form of update is a proxy for "no update". We set $F_n = 0.999$, meaning the internal model with index $i \neq m(k)$ slowly dissipates its state until the next update when again it happens that $i = m(k)$.

We begin our analysis of the model using a motor command

$$u_f(k) = u_{f,t(k)}$$
$$u(k) = u_f(k) + \psi \hat{w}_{t(k)}(k)\,,$$

where $t(k)$ is the target for the next reach, and $u_f(k)$ is the feedforward component of the motor command, constituted at the end of the kth reach in preparation for use in the next one. Here ψ represents an unknown parameter (that has been adapted a priori, hence the adaptation process is omitted). We will comment on the role of ψ below. Several observations are in order.

- The internal model output that appears in the motor command is dictated by the choice of feedforward command, $u_f(k) = u_{f,t(k)}$, which is itself determined by the choice of target for the next reach. Thus, feedforward commands and their associated internal model outputs are always paired. To say another way, it is not allowed to use a motor command $u(k) = u_{f,j} + \psi \hat{w}_i(k)$, if $i \neq j$.
- Our model dissociates the updating of an internal model from the ensuing motor command in the sense that the robot can reach for a target $t(k)$ on the next trial $k+1$, even if it takes a measurement with respect to a target $m(k) \neq t(k)$. The consequence of this is that some internal model updates are *unobservable*, possibly only to be revealed in later trials or as *aftereffects* once the experiment is concluded.

To understand why this model works, we consider a scenario that can be viewed as a typical mode of operation. Suppose the robot performs repetitive reaches to the same target $t \in \{1, \dots, N\}$ for all trials (a more general scenario with switching between targets is shown in the simulation). That is, $t(k) = t$ for some $t \in \{1, \dots, N\}$ and for all $k \geq 1$. Thus, the feedforward component of the motor command is

$$u_f(k) = u_{f,t}\,, \qquad \forall k \geq 1\,.$$

During the first $j-1$ trials, the robot also makes measurements relative to this same target. That is $m(k) = t$ for $k = 1, \dots, j-1$. Therefore, the error recorded during the first $j-1$ reaches is

$$e(k) = r_t - x(k) - d\,.$$

Using the update rules for the internal models given above, we compute the internal model update:

$$\begin{aligned}\hat{w}_t(k+1) &= Fw_{0,t}(k) + FGe(k) + Ge(k+1) + Fw_{1,t}(k) \\ &\quad + G[u(k) - u_f(k)] \\ &= Fw_{0,t}(k) + FGe(k) + G[r_t - x(k+1) - d] \\ &\quad + Fw_{1,t}(k) + G[u(k) - u_f(k)] \\ &= F\hat{w}_t(k) + G(-d)\,.\end{aligned}$$

We see that the internal model update associated with the target t is the one we expect, based on the analogous continuous-time computation (7). If $G = 1 - F$ and j is sufficiently large, then $\hat{w}_t(k)$ converges to $-d$. Meanwhile, the other internal models slowly dissipate their values; that is,

$$\hat{w}_i(k+1) = F_n \hat{w}_i(k)\,, \qquad i \in \{1, \dots, N\}\,, \qquad i \neq t\,.$$

Now suppose the robot chooses to make a measurement relative to some target $m(j) \neq t$ at trial $k = j$, such that

$$e(j) = r_{m(j)} - x(j) - d\,.$$

We want to know the effect of this "extraneous" measurement on the updates of the internal model outputs $\hat{w}_i$, $i \in \{1, \dots, N\}$. On the jth trial, the following updates occur:

$$\begin{aligned}\hat{w}_{m(j)}(j) &= w_{0,m(j)}(j) + Ge(j) + w_{1,m(j)}(j) \\ w_{0,m(j)}(j+1) &= Fw_{0,m(j)}(j) + FGe(j) \\ w_{1,m(j)}(j+1) &= Fw_{1,m(j)}(j) + G(u(j) - u_{f,m(j)})\,,\end{aligned}$$

and for all $i \in \{1, \dots, N\}$ with $i \neq m(j)$:

$$\begin{aligned}\hat{w}_i(j) &= w_{0,i}(j) + w_{1,i}(j) \\ w_{0,i}(j+1) &= F_n w_{0,i}(j) \\ w_{1,i}(j+1) &= F_n w_{1,i}(j)\,.\end{aligned}$$

Now we look at the next trial. Suppose the robot returns its attention to the original target such that $m(j+1) = t$. Therefore,

$$e(j+1) = r_t - x(j+1) - d\,.$$

Then we compute

$$\begin{aligned}
&\hat{w}_{m(j)}(j+1)\\
&\quad = w_{0,m(j)}(j+1) + w_{1,m(j)}(j+1)\\
&\quad = F[w_{0,m(j)}(j) + w_{1,m(j)}(j)] + FGe(j) + G(u(j) - u_{f,m(j)})\\
&\quad = F[w_{0,m(j)}(j) + w_{1,m(j)}(j)] + FG[r_{m(j)} - x(j) - d]\\
&\qquad + G[r_t + \psi\hat{w}_t(j) - r_{m(j)}]\\
&\quad = FF_n\hat{w}_{m(j)}(j-1) + G\psi\hat{w}_t(j) + FG[r_t - x(j) - d]\\
&\qquad + (1-F)G[r_t - r_{m(j)}]\,.
\end{aligned} \tag{17}$$

The second term contains significant information in this update. Assuming again that $G = 1 - F$ and j is sufficiently large, then $\hat{w}_t(j)$ converges to $-d$. Therefore, the term $\psi\hat{w}_t(j)$ represents a *transfer of learning* from the internal model for target t to the internal model for target $m(j)$. The parameter ψ captures the proportion of learning that is transferred, which would ideally be close to 1.

The last two terms in (17) are to be interpreted as perturbations. The third term includes the (unseen) error w.r.t. target t at trial j, namely $r_t - x(j) - d$, which becomes small as the robot continues to reach for target t. The fourth term is $G^2[r_t - r_{m(j)}]$. Typical values for the parameters are $F = 0.9$ and $G = 0.1$. Suppose the targets t and $m(j)$ are 30° apart. Then this perturbation term will have a value of 0.3. This perturbation may induce an acceptable degradation relative to the term $G\psi\hat{w}_t(j)$ if $d(k)$ is an order of magnitude larger or more. One may also devise a strategy where measurements are taken only relative to targets in contiguous adaptation fields, so that $r_t - r_{m(j)}$ is below a threshhold. In summary, the previous computation shows that, in theory, learning acquired by the internal model with index t can be transferred to the internal model with index $m(j)$.

Next, we must consider the effect of these updates on the other internal models. Thus, we compute

$$\begin{aligned}
\hat{w}_t(j+1) &= w_{0,t}(j+1) + Ge(j+1) + w_{1,t}(j+1)\\
&= w_{0,t}(j) + Ge(j+1) + w_{1,t}(j)\\
&= \hat{w}_t(j) + Ge(j+1)\,.
\end{aligned}$$

We see that this internal model experiences a perturbation $e(j+1)$ that corrupts its estimate of the disturbance d. However, if j is sufficiently long, then $e(j+1)$ is small, so this perturbation should cause a minor degradation in the next trial. Finally, for internal models with indices $i \neq t$ and $i \neq m(j)$:

$$\hat{w}_i(j+1) = w_{0,i}(j+1) + w_{1,i}(j+1) = F_n\hat{w}_i(j)\,.$$

These internal models continue to dissipate their values.

Simulation results using the model are shown in Fig. 6. Parameter values in the model are: $F = 0.95$, $G = 1 - F$, $\psi = 1$, $F_n = 0.9998$. There are three targets with horizontal angular positions $r(1) = 0$, $r(2) = 45$, and $r(3) = -20$. The handheld tool causes a disturbance in the arm position by an amount of −45°. After a baseline block of 20 trials with no tool, the robot picks up the tool and reaches for target 1 for 60 trials, then target 2 for 60 trials, and target 3 for the last 60 trials. While the robot reaches for target 1, it measures an error with respect to (w.r.t.) target 2 at the end of every 8th reach; and w.r.t. target 3 at the end of every 12th reach. We see in the right figure that the internal models begin "charging up" as they collectively estimate the disturbance induced by holding the tool. By the time the robot reaches the second target, the first internal model is almost fully charged. Only infrequent measurements are needed to retain a fresh estimate of the disturbance by this internal model. Finally, by the end of the experiment, all internal models have approached a consensus value on the disturbance induced by holding a tool. The robot may save the motor memory, so if this tool is encountered again, the revised motor commands may be immediately recalled.

The model we have presented for simple tool learning may be related to a well-known visuomotor experiment with

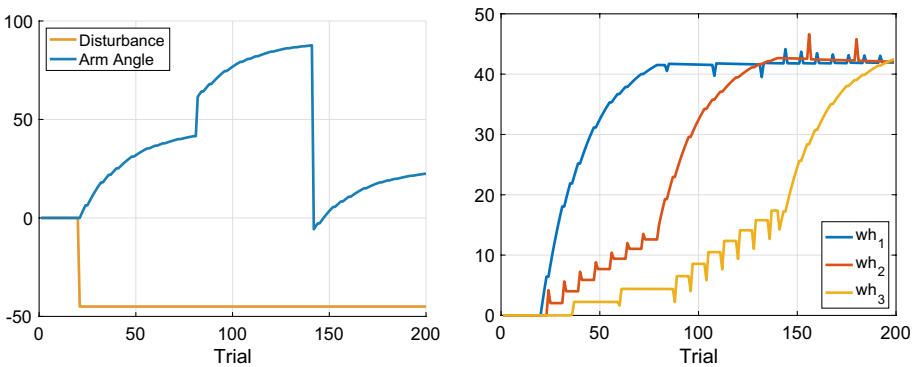

Fig. 6 A robot arm reaching for each of three targets, while occasionally glancing at the other two. The left figure shows the arm angle and the right figure shows $\hat{w}_i(k)$ for the three internal models

human subjects reported in [130]. A subject is presented with two targets separated by a fixed angle of 45°. The subject is instructed to aim for the second target at $r(2) = 45°$ while observing a cursor position on a computer screen displayed at the end of each reach. The cursor position has been rotated by $d(k) = -45°$ from the true hand angle, so that by aiming for the second target, the subject is able to make the error between the cursor and the first target at $r(1) = 0°$ be close to zero.

We can simulate this experiment using our learning model. We assume the subject aims for the second target in all trials, so $t(k) = 2$, according to the instructions of the experimenter. However, the subject occassionally shifts attention to the error formed w.r.t. the first target [131, 132]. Suppose the subject attends to the first target at the end of 20 percent of trials and to the second target in 80 percent of trials. Simulation results are shown in Fig. 7. The top figures show qualitatively the same results as obtained in [130]. The bottom figure shows the response of the internal models - both are estimating $-d(k) = 45$ (the minus sign is an artifact of our choice of parameters and is not significant). The second internal model is faster because it experiences more frequent updates. The hand angle ultimately reaches 90 to place the cursor at $r(2) = 45$, subject to the disturbance of $d(k) = -45$. The interesting behavior appears in the washout trials (the last 20 trials), when the subject again focuses on the first target at $t(1) = 0$, and we observe the aftereffects of the first internal model having charged up during the previous phase.

We conclude this section with three remarks.

(i) The fact that the models in this section do not have a component $Ke(k)$ in the motor command carries some significance that we have not expanded on. Our future work will explore the capability to enable or disable this component.

(ii) Analyses presented in this section are intended as plausibility arguments. A rigorous stability analysis using stability techniques for switched systems [133] is needed.

(iii) Despite the fact that visuomotor adaptation appears to be an ideal context for the application of reinforcement learning algorithms, the experimental evidence does not support this form of learning [134, 135]. This raises intriguing questions about why an error-driven approach may be better suited than reinforcement learning for this brain process.

Conclusion

This paper has presented an overview of results on the use of regulator theory to interpret and model the contribution of the cerebellum to motor systems. We considered the slow eye movement systems: the VOR, gaze holding, and smooth pursuit, as well as the optokinetic system. We found that using regulator theory one could derive models that are consistent with the known neural circuits and also recover the

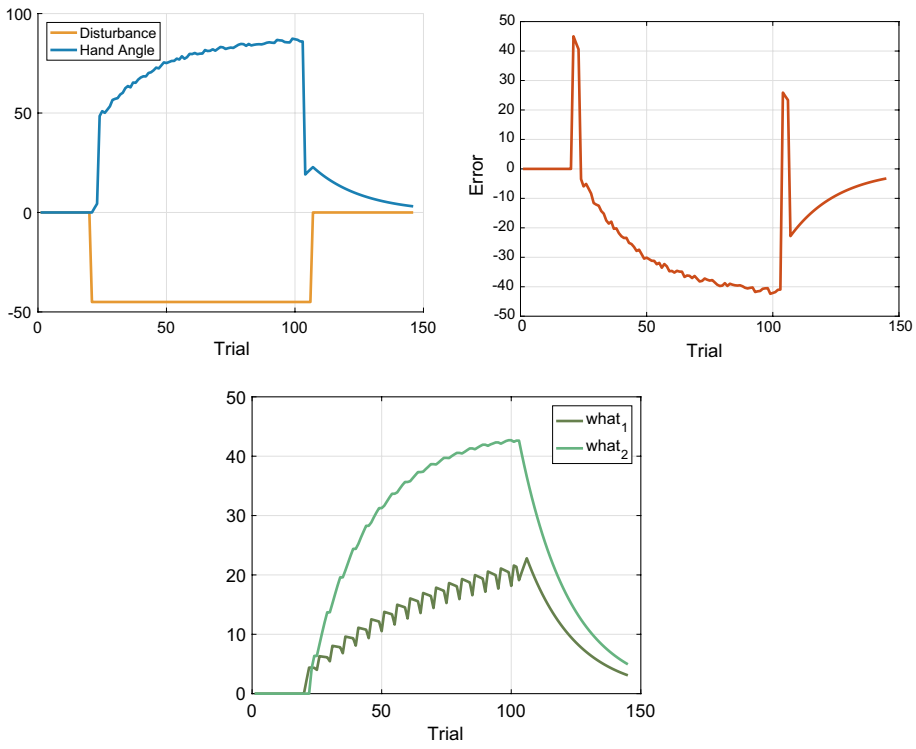

Fig. 7 Mazzoni and Krakauer's experiment. The top left figure displays the disturbance $d(k)$ and the hand angle $x(k)$ as a function of the trial number k. The top right figure shows the error $r_{t(k)} - x(k) - d$ with respect to the first target. The bottom figure shows the internal model states $\hat{w}_1(k)$, $\hat{w}_2(k)$ as a function of k

standard experimental results for those motor systems. We also surveyed results for visuomotor adaptation; despite the fact that the models are discrete-time difference equations rather than differential equations, a nearly identical methodology as in continuous time could be employed to derive a model that recovers many of the standard experimental results. A pattern in the motor systems we examined is that the cerebellum must be endowed with a special capability to enable and disable internal models without causing damage to the body. We have identified the nucleo-cortical pathway as a possible mechanism to implement this capability. Finally, the paper argues that mathematical modeling of the cerebellum can well serve as a research agenda to develop humanoid robots that possess cerebellar-like intelligences.

Our view of cerebellar function to perform disturbance rejection of exogenous signals adds to a current debate in neuroscience on whether the cerebellum contains internal models of the plant or of the environment [2–4, 136]. Also, how do so-called *forward models* contribute to the generation of internal models of either the plant or the environment [25, 26]? Ultimately, certain aspects of the debate between internal (forward) models of the plant and internal models of the environment may turn out to be semantic. Witness that, mathematically speaking, a forward model of the plant can be utilized toward disturbance rejection of signals in the environment, as we have done in our model of visuomotor adaptation [9].

Consider the study in [137] in which it is reported that the cerebellar flocculus of the monkey contains a forward model of the oculomotor plant. A monkey performs vertical smooth pursuit of a sinusoidal target that lies at a vertical eccentric position of up to 20° to the left or right of center. This means the eye is rotated from its central position to the left or right in order to foveate the vertically moving target. The mechanics of the oculomotor plant generate torsional forces that are not present in the motor command sent to the oculomotor neurons to drive the eye. These torsional forces are amplified during smooth pursuit with the eye in an eccentric position. It is observed that the mossy fibers to the cerebellum do not carry torsional information, but vertical Purkinje cells of the floccular complex do carry such information. It is proposed that the floccular complex computes an estimate of torsional eye movement since the torsional signal is present in the PCs but not the mossy fibers.

A question that must be raised is: is the output of the floccular complex purely a signature of the plant dynamics or rather a signature of the disturbance signal (a sinusoid) filtered through the oculomotor plant? In the latter case, the internal model would provide an estimate of the filtered disturbance. Strictly speaking, the internal model would not be a forward model of the plant (the brainstem neural integrator more closely resembles a forward model of the plant). We believe asking questions of this nature, both theoretically and experimentally, can help to resolve the current controversy between forward models of the plant v.s. internal models of disturbances in the cerebellum.

Acknowledgements I would like to thank my graduate students Erin Battle, Ahmad Abdel Gawad, Mohamed Hafez, and Erick Mejia Uzeda for their contributions to this research.

Data availability There is no data associated with this article.

Declarations

Conflict of interest The author has no conflict of interest.

References

1. Francis B, Wonham WM. The internal model principle of control theory. Automatica. 1976;12:457–65.
2. Lisberger S. Internal models of eye movement in the floccular complex of the monkey cerebellum. Neuroscience. 2009;162(3):763–76.
3. Miles O, Cerminara N, Marple-Horvat D. Purkinje cells in the lateral cerebellum of the cat encode visual events and target motion during visually guided reaching. J Physiol. 2006;571:619–37.
4. Cerminara N, Apps R, Marple-Horvat D. An internal model of a moving visual target in the lateral cerebellum. J Physiol. 2009;587(2):429–42.
5. Wonham WM. Linear multivariable control: a geometric approach. 3rd ed. New York: Springer; 1985.
6. Broucke ME. Model of the oculomotor system based on adaptive internal models. IFAC World Congress. 2020;53(2):16430–7.
7. Broucke ME. Adaptive internal model theory of the oculomotor system and the cerebellum. IEEE Trans Autom Control. 2021;66:5444–50.
8. Gawad A, Broucke M. Visuomotor adaptation is a disturbance rejection problem. In: IEEE Conference on Decision and Control. 2020. p. 3895–3900.
9. Hafez M, Uzeda E, Broucke M. Discrete-time output regulation and visuomotor adaptation. In: IEEE Conference on Decision and Control, 2021.
10. Battle E, Broucke ME. Adaptive internal models in the optokinetic system. In: IEEE Conference on Decision and Control, 2021.
11. Kreisselmeier G. Adaptive observers with exponential rate of convergence. IEEE Trans Autom Control. 1977;22(1):2–8.
12. Krstic M, Kanellakopoulos I, Kokotovic P. Nonlinear and adaptive control design. New York: Wiley-Interscience; 1995.
13. Fujita M. Adaptive filter model of the cerebellum. Biol Cybern. 1982;45:195–206.
14. Dean P, Porrill J. Adaptive filter models of the cerebellum: computational analysis. Cerebellum. 2008;7:567–71.
15. Dean P, Porrill J, Ekerot C-F, Jorntell H. The cerebellar microcircuit as an adaptive filter: experimental and computational evidence. Nat Rev Neurosci. 2010;11:30–45.
16. Ruigrok T. Ins and outs of cerebellar modules. Cerebellum. 2011;10:464–74.
17. Houck B, Person A. Cerebellar loops: a review of the nucleocortical pathway. Cerebellum. 2014;13:378–85.
18. Ito M. The cerebellum and neural control. New York: Raven Press; 1984.
19. Broucke ME. On the use of regulator theory in neuroscience with implications for robotics. In: Proc. 18th International Conference

on Informatics in Control, Automation and Robotics. 2021. p. 11–23.
20. Imamizu H, Kuroda T, Miyauchi S, Yoshioka T, Kawato M. Modular organization of internal models of tools in the human cerebellum. Proc Natl Acad Sci. 2003;100(9):5461–6.
21. Ito M. Bases and implications of learning in the cerebellum-adaptive control and internal model mechanism. Prog Brain Res. 2005;148:95–109.
22. Miall R, Weir D, Wolpert D, Stein J. Is the cerebellum a smith predictor? J Mot Behav. 1993;25(3):203–16.
23. Miall RC, Wolpert DM. Forward models for physiological motor control. Neural Netw. 1996;9(8):1265–79.
24. Porrill J, Dean P, Anderson SR. Adaptive filters and internal models: multilevel description of cerebellar function. Neural Netw. 2013;47:134–49.
25. Tanaka H, Ishikawa T, Lee J, Kakei S. The cerebro-cerebellum as a locus of forward model: a review. Front Syst Neurosci. 2020;14:19. https://doi.org/10.3389/fnsys.2020.00019.
26. Welniarz Q, Worbe Y, Gallea C. The forward model: a unifying theory for the role of the cerebellum in motor control and sense of agency. Front Syst Neurosci. 2021;14(19).
27. Wolpert D, Miall C, Kawato M. Internal models in the cerebellum. Trends Cogn Sci. 1998;2(9):338–47.
28. Eccles J, Ito M, Szentagothai J. The cerebellum as a neuronal machine. Berlin: Springer; 1967.
29. Apps R, Hawkes R, et al. S.A.: Cerebellar modules and their role as operational cerebellar processing units. Cerebellum. 2018;17:654–82.
30. Ioannou P, Sun J. Robust adaptive control. New York: Dover; 2012.
31. Oja E. A simplified neuron model as a principle component analyzer. J Math Biol. 1982;15:267–73.
32. Sejnowski TJ. Storing covariance with nonlinearly interacting neurons. J Math Biol. 1977;4:303–21.
33. Dayan P, Abbott L. Theoretical neuroscience: computational and mathematical modeling of neural systems. Cambridge: The MIT Press; 2001.
34. Kleim JA, Jones TA. Principles of experience-dependent neural plasticity: implications for rehabilitation after brain damage. J Speech Lang Hear Res. 2008;51(1):S225–39.
35. Uzeda EM, Broucke ME. Robust parameter adaptation and the μ-modification. Syst Control Lett. 2023;171: 105416.
36. Uzeda EM, Broucke ME. Adaptive output regulation and the use it or lose it principle. In: IEEE Conference on Decision and Control, 2023.
37. Morehead R, Taylor J, Parvin D, Ivry R. Characteristics of implicit sensorimotor adaptation revealed by task-irrelevant clamped feedback. J Cogn Neurosci. 2017;29(6):1061–74.
38. Kim HE, Morehead JR, Parvin DE, et al. Invariant errors reveal limitations in motor correction rather than constraints on error sensitivity. Commun Biol. 2018;1:19. https://doi.org/10.1038/s42003-018-0021-y.
39. Morton S, Bastian A. Cerebellar control of balance and locomotion. Neuroscientist. 2004;10(3):247–59.
40. Morton S, Bastian A. Cerebellar contributions to locomotion adaptations during splitbelt treadmill walking. J Neurosci. 2006;26(36):9107–16.
41. Fairhurst D, Tyukin I, Nijmeijer H, van Leeuwen C. Observers for canonic models of neural oscillators. Math Model Nat Phenom. 2010;5(2):146–84.
42. Byrnes C, Priscoli FD, Isidori A. Output regulation of uncertain nonlinear systems. Boston: Birkhauser; 1997.
43. Huang J. Nonlinear output regulation. Philadelphia: Society for Industrial and Applied Mathematics; 2004.
44. Isidori A. Nonlinear control system. London: Springer; 1995.
45. Isidori A. Lectures in feedback design for multivariable systems. Switzerland: Springer; 2017.
46. Nikiforov V, Gerasimov D. Adaptive regulation, vol. 491. Switzerland: Springer; 2022.
47. Serrani A, Isidori A, Marconi L. Semi-global nonlinear output regulation with adaptive internal model. IEEE Trans Autom Control. 2001;46(8):1178–94.
48. Messineo S, Serrani A. Adaptive feedforward disturbance rejection in nonlinear systems. Syst Control Lett. 2009;58:576–83.
49. Cao C, Annaswamy AM, Kojic A. Parameter convergence in nonlinearly parametrized systems. IEEE Trans Autom Control. 2003;48(3):397–411.
50. Kojic A, Annaswamy AM. Adaptive control of nonlinearly parameterized systems with a triangular structure. Automatica. 2002;38(1):115–23.
51. Tyukin IY, Prokhorov DV, Terekhov VA. Adaptive control with nonconvex parameterization. IEEE Trans Autom Control. 2003;48(4):554–67.
52. Tyukin IY, Prokhorov DV, van Leeuwen C. Adaptation and parameter estimation in systems with unstable target dynamics and nonlinear parametrization. IEEE Trans Autom Control. 2007;52(9):1543–59.
53. Bastin G, Gevers MR. Stable adaptive observers for nonlinear time-varying systems. IEEE Trans Autom Control. 1988;33(7):650–8.
54. Marino R, Tomei P. Global adaptive observers for nonlinear systems via filtered transformations. IEEE Trans Autom Control. 1992;37(8):1239–45.
55. Marino R, Tomei P. Adaptive observers with arbitrary exponential rate of convergence for nonlinear systems. IEEE Trans Autom Control. 1995;40(7):1300–4.
56. Tomei P, Marino R. An enhanced feedback adaptive observer for nonlinear systems with lack of persistency of excitation. IEEE Trans Autom Control. 2023;68(8):5067–72. https://doi.org/10.1109/TAC.2022.3214798.
57. Tyukin IY, Steur E, Nijmeijer H, van Leeuwen C. Adaptive observers and parameter estimation for a class of systems nonlinear in the parameters. Automatica. 2013;49(8):2409–23.
58. Robinson D. The use of control systems analysis in the neurophysiology of eye movements. Annu Rev Neurosci. 1981;4(1):463–503.
59. Leigh R, Zee D. The neurology of eye movements. 5th ed. New York: Oxford University Press; 2015.
60. Carpenter R. Cerebellectomy and the transfer function of the vestibulo-ocular reflex in the decerebrate cat. Proc Roy Soc Lond Ser B Biol Sci. 1972;181(1065):353–74.
61. Guthrie B, Porter J, Sparks D. Corollary discharge provides accurate eye position information to the oculomotor system. Science. 1983;221:1193–5.
62. Keller E, Robinson D. Absence of a stretch reflex in extraocular muscles of the monkey. J Neurophysiol. 1971;34(5):908–19.
63. Glasauer S. Cerebellar contribution to saccades and gaze holding. Ann NY Acad Sci. 2003;1004(1):206–19.
64. Blohm G, Missal M, Lefevre P. Direct evidence for a position input to the smooth pursuit system. J Neurophysiol. 2005;94:712–21.
65. Bahill A, McDonald J. Model emulates human smooth pursuit system producing zero-latency target tracking. Biol Cybern. 1983;48:213–22.
66. Bahill A, McDonald J. Smooth pursuit eye movements in response to predictable target motions. Vis Res. 1983;23(12):1573–83.
67. Robinson D, Gordon J, Gordon S. A model of the smooth pursuit eye movement system. Biol Cybern. 1986;55:43–57.
68. Pola J, Wyatt H. Target position and velocity: the stimulus for smooth pursuit eye movement. Vis Res. 1980;20:523–34.

69. Pola J. Models of the saccadic and smooth pursuit systems. New York: Springer; 2002. p. 385–429.
70. Wyatt H, Pola J. Smooth pursuit eye movements under open-loop and closed-loop conditions. Vis Res. 1983;23(10):1121–31.
71. Brostek L, Eggert T, Glasauer S. Gain control in predictive smooth pursuit movements: evidence for an acceleration-based predictive mechanism. eNeuro. 2017;4(3):1–13.
72. Deno D, Crandall W, Sherman K, Keller E. Characterization of prediction in the primate visual smooth pursuit system. Biosystems. 1995;34:107–28.
73. Yasui S, Young L. On the predictive control of foveal eye tracking and slow phases of optokinetic and vestibular nystagmus. J Physiol. 1984;347:17–33.
74. de Xivry J-JO, Coppe S, Blohm G, Lefevre P. Kalman filtering naturally accounts for visually guided and predictive smooth pursuit dynamics. J Neurosci. 2013;33(44):17301–13.
75. Zee D, Yamazaki A, Butler P, Gucer G. Effects of ablation of flocculus and paraflocculus on eye movements in primate. J Neurophysiol. 1981;46(4):878–99.
76. Cullen K, Brooks J, Jamali X, Carriot J, Massot C. Internal models of self-motion: computations that suppress vestibular reafference in early vestibular processing. Exp Brain Res. 2011;210:377–88.
77. Roy J, Cullen K. Vestibuloocular reflex signal modulation during voluntary and passive head movement. J Neurophysiol. 2002;87:2337–57.
78. Roy J, Cullen K. Brain stem pursuit pathways: dissociating visual, vestibular, and proprioceptive inputs during combined eye-head gaze tracking. J Neurophysiol. 2003;90(1):271–90.
79. Dean P, Porrill J, Stone J. Decorrelation control by the cerebellum achieves oculomotor plant compensation in simulated vestibulo-ocular reflex. Roy Soc. 2002;269:1895–904.
80. Büttner U, Waespe W. Purkinje cell activity in the primate flocculus during optokinetic stimulation, smooth pursuit eye movements, and vor-suppression. Exp Brain Res. 1984;55:97–104.
81. Keller E, Daniels P. Oculomotor related interaction of vestibular nucleus cells in alert monkey. Exp Neurol. 1975;46:187–98.
82. McIntyre J, Zago M, Berthoz A, Lacquantini F. Does the brain model newton's laws? Nat Neurosci. 2001;4(7):693–4.
83. Zago M, Lacquaniti F. Visual perception and interception of falling objects: a review of evidence for an internal model of gravity. J Neural Eng. 2005;2:198–208.
84. Zago M, McIntyre J, Senot P, Lacquaniti F. Internal models and prediction of visual gravitational motion. Vis Res. 2008;48(14):1532–8.
85. Baumann O, Borra R, Bower J, et al. Consensus paper: the role of the cerebellum in perceptual processes. Cerebellum. 2015;14:197–220.
86. MacKay WA, Murphy JT. Cerebellar modulation of reflex gain. Prog Neurobiol. 1979;13(4):361–417.
87. Roy J, Cullen K. Dissociating self-generated from passively applied head motion: neural mechanisms in the vestibular nuclei. J Neurosci. 2004;24(9):2102–11.
88. Cullen K. The neural encoding of self-motion. Curr Opin Neurobiol. 2011;21:587–95.
89. Rochefort C, Arabo A, Andre M, Poucet B, Save E, Rondi-Reig L. Cerebellum shapes hippocampal spatial code. Science. 2011;334:385–9.
90. Brooks J, Cullen K. The primate cerebellum selectively encodes unexpected self-motion. Curr Biol. 2013;23:947–55.
91. Merfeld D, Zupan L, Peterka R. Humans use internal models to estimate gravity and linear acceleration. Nature. 1999;398:615–8.
92. Angelaki D, Shaikh A, Green A, Dickman J. Neurons compute internal models of the physical laws of motion. Nature. 2004;430:560–4.
93. Laurens J, Meng H, Angelaki D. Neural representation of orientation relative to gravity in the macaque cerebellum. Neuron. 2013;80:1508–18.
94. Angelaki D, Hess B. Lesion of the nodulus and ventral uvula abolish steady-state off-vertical axis otolith response. J Neurophysiol. 1995;73(4):1716–20.
95. Optican LM, Robinson DA. Cerebellar-dependent adaptive control of primate saccadic system. J Neurophysiol. 1980;44(6):1058–76.
96. Cassanello C, Ohl S, Rolfs M. Saccadic adaptation to a systematically varying disturbance. J Neurophysiol. 2016;116:336–50.
97. Bell C. Evolution of cerebellum-like structures. Brain Behav Evol. 2002;59:312–26.
98. Bastian J. Plasticity in an electrosensory system. I. General features of dynamic sensory filter. J Neurophysiol. 1996;76:2483–96.
99. Bodznick D, Montgomery J, Carey M. Adaptive mechanisms in the elasmobranch hindbrain. J Exp Biol. 1999;202:1357–64.
100. Sawtell N, Williams A. Transformations of electrosensory encoding associated with an adaptive filter. J Neurosci. 2008;28(7):1598–612.
101. Uzeda EM, Broucke ME. Training reflexes using adaptive feedforward control. IEEE Open Access Control J. (Accepted September 2023).
102. Broucke ME. Adaptive internal models in neuroscience. Found Trends Syst Control. 2022;9(4):365–550.
103. Sylvestre P, Cullen K. Quantitative analysis of abducens neuron discharge dynamics during saccadic and slow eye movements. J Neurophysiol. 1999;82(5):2612–32.
104. Robinson D. The effect of cerebellectomy on the cat's vestibulo-ocular integrator. Brain Res. 1974;71(2):195–207.
105. Galiana H, Outerbridge J. A bilaternal model for central neural pathways in vestibuloocular reflex. J Neurophysiol. 1984;51(2):210–41.
106. Büttner U, Büttner-Ennever J. Present concepts of oculomotor organization. Prog Brain Res. 2006;151:1–42.
107. Ramanchandran R, Lisberger S. Neural substrate of modified and unmodified pathways for learning in monkey vestibuloocular reflex. J Neurophysiol. 2008;100:1868–78.
108. Serrani A, Isidori A. Semiglobal nonlinear output regulation with adaptive internal model. In: IEEE Conference on Decision and Control. 2000. p. 1649–54.
109. Barnes G, Goodbody S, Collins S. Volitional control of anticipatory ocular pursuit responses under stabilized image conditions in humans. Exp Brain Res. 1995;106:301–17.
110. Morris E, Lisberger S. Different responses to small visual errors during initiation and maintenance of smooth-pursuit eye movements in monkeys. J Neurophysiol. 1987;58(6):1351–69.
111. Stone L, Lisberger S. Visual responses of Purkinje cells in the cerebellar flocculus during smooth-pursuit eye movements in monkeys. I. Simple spikes. J Neurophysiol. 1990;63(5):1241–61.
112. Churchland M, Chou I, Lisberger S. Evidence for object permanence in the smooth-pursuit eye movements of monkeys. J Neurophysiol. 2003;90:2205–18.
113. Narendra K, Annaswamy A. Stable adaptive systems. New York: Dover Publications; 1989.
114. Wolpert D, Kawato M. Multiple paired forward and inverse models for motor control. Neural Netw. 1998;11(7):1317–29.
115. Cohen B, Matsuo V, Raphan T. Quantitative analysis of the velocity characteristics of optokinetic nystagmus and optokinetic after-nystagmus. J Physiol. 1977;270:321–44.

116. Raphan T, Matsuo V, Cohen B. Velocity storage in the vestibulo-ocular reflex arc (VOR). Exp Brain Res. 1979;35:229–48.
117. Waespe W, Henn V. Conflicting visual-vestibular stimulation and vestibular nucleus activity in alert monkeys. Exp Brain Res. 1978;33:203–11.
118. Waespe W, Henn V. Reciprocal changes in primary and secondary optokinetic after-nystagmus (OKAN) produced by repetitive optokinetic stimulation in the monkey. Archiv Psychiatrie und Nervenkrankheiten. 1978;225:23–30.
119. Büttner U, Waespe W, Henn V. Duration and direction of optokinetic after-nystagmus as a function of stimulus exposure time in the monkey. Arch Psychiat Nervenkr. 1976;222:281–91.
120. Miki S, Urase K, Baker R, et al. Velocity storage mechanism drives a cerebellar clock for predictive eye velocity control. Sci Rep. 2020;10:6944. https://doi.org/10.1038/s41598-020-63641-0.
121. Kojima Y, Iwamoto Y, Yoshida K. Memory of learning facilitates saccadic adaptation in the monkey. J Neurosci. 2004;24(34):7531–9.
122. Smith MA, Ghazizadeh A, Shadmehr R. Interacting adaptive processes with different timescales underlie short-term motor learning. PLOS Biol. 2006;4(6). https://doi.org/10.1371/journal.pbio.0040179.
123. Shadmehr R, Wise S. The computational neurobiology of reaching and pointing. Cambridge: MIT Press; 2005.
124. Martin T, Keating J, Goodkin H, Bastian A, Thach W. Throwing while looking through prisms. II. Specificity and storage of multiple gaze-throw calibrations. Brain. 1996;119:1199–211.
125. Galea J, Vazquez A, Pasricha N, de Xivry J, Celnik P. Dissociating the roles of the cerebellum and motor cortex during adaptive learning: the motor cortex retains what the cerebellum learns. Cereb Cortex. 2011;21:1761–70.
126. Kitago T, Ryan S, Mazzoni P, Krakauer J, Haith A. Unlearning versus savings in visuomotor adaptation: comparing effects of washout, passage of time, and removal of errors on motor memory. Front Hum Neurosci. 2013;7. https://doi.org/10.3389/fnhum.2013.00307.
127. Bond K, Taylor J. Flexible explicit but rigid implicit learning in a visuomotor adaptation task. J Neurophysiol. 2015;113:3836–49.
128. Shmuelof L, Hang V, Haith A, Dekicki R, Mazzoni P, Krakauer J. Overcoming motor forgetting through reinforcement of learned actions. J Neurosci. 2012;32:14617–21.
129. Vaswani P, Shmuelof L, Haith A, Deknicki R, Huang V, Mazzoni P, Shadmehr R, Krakauer J. Persistent residual errors in in motor adaptation tasks: reversion to baseline and exploratory escape. J Neurosci. 2015;35(17):6969–77.
130. Mazzoni P, Krakauer J. An implicit plan overrides an explicit strategy during visuomotor adaptation. J Neurosci. 2006;26:3642–5.
131. Rand M, Rentsch S. Gaze locations affect explicit process but not implicit process during visuomotor adaptation. J Neurophysiol. 2015;113:88–99.
132. de Brouwer A, Albaghdadi M, Flanagan J, Gallivan J. Using gaze behavior to parcellate the explicit and implicit contributions to visuomotor learning. J Neurophysiol. 2018;120:1602–15.
133. Liberzon D. Switching in systems and control. Boston: Birkhauser; 2003.
134. Izawa J, Shadmehr R. Learning from sensory and reward prediction errors during motor adaptation. PLoS Comput Biol. 2011;7(3):1–11. https://doi.org/10.1371/journal.pcbi.1002012.
135. Spampinato D, Celnik P. Multiple motor learning processes in humans: their neurophysiological bases. Neuroscientist. 2021;27(3):246–67.
136. Blazquez P, Kim GT, Yakusheva T. Searching for an internal representation of stimulus kinematics in the response of ventral paraflocculus purkinje cells. Cerebellum. 2017;16:817–26.
137. Kim G, Laurens J, Yakusheva TA, Blazquez PM. The macaque cerebellar flocculus outputs a forward model of eye movement. Front Integr Neurosci. 2019;13. https://doi.org/10.3389/fnint.2019.00012.